TECHNOLOGY
UTILIZATION REPORT

NON-GLASSY
INORGANIC FIBERS
AND COMPOSITES

by
CAMERON G. HARMAN

NATIONAL AERONAUTICS AND SPACE ADMINISTRATION

Washington, D. C.   August 1966

NOTICE

This document was prepared under the sponsorship of the National Aeronautics and Space Administration. Neither the United States Government nor any person acting on behalf of the United States Government assumes any liability resulting from the use of the information contained in this document, or warrants that such use will be free from privately owned rights.

Foreword

The Technology Utilization Division of the National Aeronautics and Space Administration issues reports, surveys, and bibliographies to make the findings of participants in space programs widely available. These publications are intended to help American industry benefit from advances that requirements for space missions have accelerated.

New materials and new combinations of materials have been needed in spacecraft. Many of them also can be used advantageously elsewhere. This report on non-glassy inorganic fibers and composites is one of several reports on materials science and engineering. It was prepared by Dr. C. G. Harman, senior research engineer in the Department of Materials Engineering at the Southwest Research Institute, with the help of NASA personnel, contractors, and other participants in the development of such fibers and composites.

GEORGE J. HOWICK, Director,
Technology Utilization Division,
National Aeronautics and Space Administration

CONTENTS

Introduction

The thermal and stress problems associated with space applications demand new materials and combinations of materials with properties markedly superior to those conventionally available. A dire need exists for high-strength, high-elastic modulus, lightweight materials. Progress is now being made toward meeting these goals through approaches based on the development and use of composites having properties which no single material has. As much as 80 percent reduction in weight may result from the use of ultra-strong filaments as reinforcements in a composite material. This report will present information about non-metallic, inorganic whiskers and fibers, and composites based on them that may be useful to industry.

Conventional materials for high-temperature applications have been developed almost to the limit of their mechanical properties' potentialities. It appears that potential high-temperature strengths of fiber-reinforced metals may be an order of magnitude greater than possible with state-of-the-art materials, and operating temperatures may be increased by as much as 2000° F.

Many applications are visualized for strong fibers, whiskers, and filaments. In the forefront is fiber reinforcement in metals, plastics, and ceramics. Numerous specific, conventional applications are visualized, such as electrical contacts, papers, filters, fabrics, spring contact components, and superstrength lightweight metals for high temperatures and insulation.

Extensive reviews of whisker technology and fiber-reinforced metals have been published, among which are reviews of fiber-reinforced metals by Machlin,[1] Baskey,[2] Kelly and Davies,[3] Cratchley,[4] and Weeton.[40]

This report will present NASA-generated information, but will refer to associated works where they impinge and interrelate. Organic and glass fibers, and compositions with organic matrices will be considered here. Extensive literature on glass-fiber-reinforced plastics and work with fiber-reinforced ceramics is referred to by Moore et al.,[5] and Carroll-Porczynski.[6]

The field of fibers and fiber reinforcement covers a wide range of disciplines. There are many separate areas of research, ranging from theories of reinforcement; fabrication of reinforced composites; the growth and preparation of whiskers and fibers; basic properties of fibers and whiskers; and physiochemical aspects of interfaces, through to engineering applications, design, and production. Several detailed approaches to the accomplishment of desired results include mechanical mixing, followed by sintering (as in cermets[7]), dispersion hardening (as in SAP[8]), and dispersion-strengthened nickel,[9] as well as fiber reinforcement. Each system has potential advantages and disadvantages. Since cermets and dispersion-strengthening[10] have been extensively reviewed elsewhere, only fibers and fiber reinforcement will be discussed in this report.

General Summary of Fibers and Filaments

GENERAL CLASSES

Inorganic fibers are classified in this report as follows:

Type	Example
Metal wires	Small cross-section wire
Glass	Fiber glass and rock wool
Ceramic	Polycrystalline oxides
Natural mineral	Asbestos; wollastonite
Synthetic mineral	Potassium titanate
Whiskers	Sapphire; boron carbide
Vapor-deposits on wire	Boron on tungsten

Metal wires, glass fiber, and vapor-deposits on wires are commonly produced as continuous filaments. Polycrystalline ceramic filaments, produced by the extrusion or drawing of ceramic-filled polymers, are reputed possible in the form of continuous filaments, but the sintered products are usually short and friable.

Polycrystalline fibers of metal and of ceramic, including those vapor-deposited on wire, undergo grain-growth at high temperatures, resulting in characteristic embrittlement and strength loss. Most acicular crystals of natural and synthetic minerals are relatively small and short, and frequently their strength potentialities have not been characterized. Synthetic whiskers tend to be single crystals of a high degree of perfection with very high strengths.

The strengths of fibers and whiskers depend upon (a) inherent strength potentialities of the material, (b) dimensions of their cross-sections, (c) morphology, and (d) for whiskers, the degree of crystal perfection and crystallographic orientation. Before discussing the strengths of fibers and whiskers, it is instructive to scan table I on relevant bulk material (Hoffman[11]). The tensile strengths and moduli of elasticity of whiskers and filaments are much greater than respective values of bulk material, which is the primary reason for their being of interest.

STRENGTH POTENTIALITIES

The strength of whiskers having diameters in the micron range is one or more orders of magnitude higher than that of respective bulk crystals. In 1952, Herring and Galt[12] demonstrated that whiskers of tin had strengths approaching theoretical values. Since that time, interest in whiskers as strengthening agents has grown. Whiskers of silicon carbide and sapphire tend to approach the following limit:

$$S = \frac{3 \times 10^2}{d}$$

Where S is tensile strength in psi, and d is in inches.*

Whiskers have strengths of $\frac{E}{10}$ to $\frac{E}{40}$, where E is Young's modulus.[13, 14] Tensile strength of bulk glass has been reported in similar terms,[15] provided specimen surfaces were perfect. This qualification is critical, and high strengths have been observed on various crystals[16, 17] that can be maintained even in samples having internal defects and dislocations.[18] Thus, tensile strengths of crystals and, consequently, of whiskers, may be anticipated. Those with high values of Young's modulus can be expected to have tensile strengths approaching values of $\frac{E}{10}$, as pointed out in 1921 by Polanyi,[19] and subsequently by others.

Whiskers having good surfaces and high hardness values probably will have high tensile strengths. Crystals with covalent bonds usually

*Harman, C. G.: Unpublished data, Southwest Research Institute, San Antonio, Texas (1964).

TABLE I.—*Physical Data on Bulk Materials of Interest*

Material		Density lb/in.^{3}	Modulus of Elasticity at 70°F, psi	$\left[\dfrac{\text{Modulus}}{\text{Density}}\right]$ inch	Melting or Decomposition Temperature, °F
Beryllium	Be	0.066	44 x 10^6	6.65 x 10^8	2340
Boron	B	0.083	50	6.03	4200
Carbon	C	0.08	2.3	0.3	7500
Columbium	Cb	0.310	23	0.74	4400
Molybdenum	Mo	0.0369	52	1.41	4800
Tantalum	Ta	0.601	27	0.45	5450
Tungsten	W	0.697	52	0.74	6170
Aluminum Oxide	Al$_2$O$_3$	0.137	60	5.0	3660
Beryllium Carbide	Be$_2$C	0.088	45	5.08	3800
Beryllium Oxide	BeO	0.103	55	5.33	4580
Boron Carbide	B$_4$C	0.091	65	7.15	4500
Magnesium Oxide	MgO	0.129	12	0.93	5070
Molybdenum Carbide	Mo$_2$C	0.320	33	1.03	4870
Silicon Carbide	SiC	0.115	70	6.10	4350
Silicon Dioxide (glass)	SiO$_2$	0.083	11	1.32	3150
Tantalum Carbide	TaC	0.523	42	0.80	7020
Titanium Carbide	TiC	0.178	51	2.85	5700
Titanium Dioxide	TiO$_2$	0.170	14	0.82	3330
Thorium Oxide	ThO$_2$	0.346	21	0.61	5900
Tungsten Carbide	WC	0.567	102.5	1.81	5030
Zirconium Carbide	ZrC	0.242	49	2.02	6400
Zirconium Oxide	ZrO$_2$	0.193	35	1.87	4700
Zirconium Silicate	ZrO$_2$·SiO$_2$	0.154	24	1.56	4600

have high ratios of hardness to modulus of elasticity. These seem to have low atomic numbers and include many carbides, borides, and some silicides and nitrides; also included are the more refractory oxides of elements of Groups III and IV of the Periodic Table. Ionic crystals of oxides of elements having large ionic radii tend to be easily weakened by dislocations, but are usually not of high hardness.

WHISKERS

Acicular growths of crystals of the variety commonly called whiskers have long been known. Whisker-like growths of silver were reported by Ercker[20] in 1574. The variety and scope of observations made on whiskers are considerable. Several excellent summary and review articles available include treatments by Brenner,[13] Coleman,[14] Gilman,[21] Nadgornyi,[22] and Hardy.[23]

Whiskers may be grown from melts or supersaturated gas phases, from solutions by chemical decomposition and electrolysis, or by growth from a solid. The resulting whiskers characteristically tend to have a high degree of crystal perfection and great strength. Whisker diameters can vary from submicron diameters to several millimeters; most are single crystals with their principal geometric axis parallel to a predominant crystallographic direction. Whiskers having diameters in the micron range may be up to two orders of magnitude stronger than bulk crystals.

THEORY OF GROWTH FROM VAPOR

Some general theories applicable to whisker growth from vapor have been advanced by Brewer and Searcy,[24] Cunningham,[25] Blakely and Jackson,[26] Wagner and Ellis,[27] and Burton et al.[28] Theoretically, whisker growth from vapor occurs in three distinguishable steps: (1) absorption from the vapor on perfect surfaces of the growing crystallite; (2) migration of the atom species to the crystallite tip, probably by surface diffusion; and (3) deposition at a tip, incorpo-

rating with that a mechanism associated with an axial screw dislocation. Each of the above steps has been verified for some whisker species.

THEORY OF SOLID-STATE GROWTH

Theories of whisker growth from metallic substrates are based upon dislocations in the surface of the substrate having a Burgers vector normal to the surface. A mechanism is required for the generation and transport of the vacancies. Theories with respect to energy for the driving force vary in detail. A situation exists where surface-free energy could be derived from reduction of strain-free energy in the substrate. Part of the driving force appears to have been derived from oxidation,[29, 30] where mechanisms are active while the whiskers are under tensile stress. The rate of growth is controlled by diffusion of vacancies to the surface, and oxidation provides the stresses for continuation of the dislocation mechanism.

GROWTH BY REDUCTION

Direct growth by the reduction of halides has been frequently practiced. Theories of growth mechanisms are similar to those proposed for growth from vapor and growth in the solid state, modified to apply to vapor reduction. This requires, in part, transport and diffusion processes involving liquid or vapor-phase halide. It is assumed that reduction is catalyzed by the growth step so that metal atoms can be directly incorporated into the growing whisker. It is further assumed that the liquid halide diffuses from the sides of the whisker to its tip.

GROWTH FROM SOLUTION

Again, theories of whisker growth from solution closely resemble those from vapor and include processes of solid-state growth. Frequently, the screw-dislocation mechanism has been considered necessary, with the assumption that supersaturation is too low for growth on side surfaces, due to two-dimensional nucleation. Electrolytic and electrolysis processes can result in whisker growth, with such growths regarded as special cases of growth from solution. Price et al.[31] proposed

that impurity effects must be included in the mechanism.

IMPURITIES

This subject is complicated and varied in detail. Impurities have an effect on the growth of whiskers and, in some cases, are known to play an essential role in their growth. Adsorbed impurities, as well as internal trace impurities, are important. For example, compositional differences at the whisker tip and on side surfaces are both theoretically and practically present in some species. Some materials, while of very high purity in final form, seem to require some impurities in the growth mechanism. Although additional experimental details are required for theoretical evaluation and correlation, a detailed discussion is irrelevant here.

EXPERIMENTAL GROWTH

Observations have been reported on an enormous variety of whiskers. They have been grown from plated substrates and alloys, and low-melting-point materials have been used to produce whiskers at reaction temperatures as low as −40°C. Among the metals successfully converted to whiskers at temperatures well below their melting points are gold, zinc, tin, platinum, and antimony.

By using the process of condensation from vapors, many pure metals have been produced in whisker form. The most successful results have been from metals of high vapor pressure, but whiskers have been prepared from metals of both high and low vapor pressures, using both inert atmospheres and vacuum.

High temperature reduction of salts with hydrogen is a method widely employed for producing whiskers.[13] Whiskers of silver [32] and lead [33] have been prepared by electrolysis methods. The general theory of growth by electrolysis was presented by Vermilyea.[34]

Among the oxides prepared as whiskers are CuO, ZnO, NiO, MgO, $MgO \cdot Al_2O_3$, $2MgO \cdot SiO_2$, Cr_2O_3, Al_2O_3, ThO_2, B_4C, BeO, Fe_2O_3, and Sb_2O_3. Many preparations can be made by heating the metal in suitable atmospheres, including wet hydrogen, moist inert gases, or air. Pfefferkorn [35]

published information on needle-growths of various oxides. Sapphire whiskers have been prepared and discussed by many, and are now available commercially.

Metallic salts of many varieties can be prepared as whiskers. Recently, the process for the growth of whiskers of silicon and germanium was described by Wagner and Ellis.[27] Whiskers of graphite, silicon carbide, and sapphire have been reported in considerable detail.

PROPERTIES

Some nominal properties of whiskers are shown in table II. Whiskers became of interest primarily because of their extremely high tensile strengths. Other properties of interest are mechanical, surface, magnetic, and electrical.

STRESS-STRAIN BEHAVIOR

Characteristically, whiskers have a large elastic region. Brenner[13] reported elastic strain data for 24 different materials, among which were iron, zinc, Al_2O_3 and SiO_2, with strains of 4.9, 2.0, 3.0, and 5.2 percent, respectively. It appears that stress-strain curves for rapid strain rates tend to be reversible, in contrast with irreversibility for slow rates. Some whiskers fracture immediately following the elastic region, but others have sharp yield points, followed by a large plastic flow region.

When tested, many whiskers show ultimate tensile strengths falling within less than one order of magnitude of the calculated theoretical values for ideal crystals. There is a tendency now to ascribe this partly to a high degree of crystal perfection, at least for Al_2O_3. However, there is a large scatter in the reported yield strengths and

ultimate strengths of whiskers. To date, no specific reasons for this scatter have been determined. Further work is needed on the causes for failure of whiskers under tensile loading.

Creep and fatigue investigations have been carried out on iron, zinc, copper, and silicon whiskers, which were reviewed by Coleman.[14] In some specimens, the creep was found to be due to dislocations that may move under stress and either reach the surface or be pinned on impurities. It has been established that fatigue does occur, but there is not sufficient evidence to clearly detail the mechanism.

FACTORS INFLUENCING STRENGTH

The major factors affecting mechanical strength of whiskers have been investigated, using the better-known species. Strength is influenced by temperature, time, surface conditions, surface films or corrosion, crystallographic orientation, impurities, and testing techniques.

Because of the interest in whiskers for reinforcement in composites for load-bearing components at high temperature, the effect of temperature on stress-strain behavior is important. Extensive work has been done at the low end of the high-temperature range, but not so much in the moderate and high-temperature ranges. Some whiskers have been examined at very low temperatures, but not exhaustively, while sapphire, silicon carbide, and boron fibers have been evaluated at the higher temperatures. Mechanical properties of some whiskers were reviewed in detail by Nadgornyi.[22]

The effects of oxide films on metallic whiskers, examined by some workers,[13] seem specific, and generalized conclusions are not warranted. The

TABLE II.—*Nominal Mechanical and Physical Properties of Whiskers*

Material	Tensile Strength (σ_t) lb/in.$^2 \times 10^{-6}$	Young's Modulus (E) lb/in.$^2 \times 10^{-6}$	Specific Gravity (S) lb/in.$^2 \times 10^{-6}$	$\dfrac{(\sigma_t)}{(S)}$ inch	$\dfrac{(E)}{(S)}$ inch
Graphite	3.0	--	137	21,700	-------
Al_2O_3	3.0	76	250	12,000	300,000
Iron	1.8	28	485	3,700	58,000
Si_3N_4	2.0	55	193	10,000	285,000
SiC	3.0	70	187	16,000	380,000
Si	1.1	26	143	7,000	182,000

·influence of impurities on simple crystals has been studied in some detail, but most of the general conclusions appear to deal with their effects on dislocations. The influence on strength is of major importance; where whiskers are to be used as reinforcement in metallic composites for high-temperature applications, diffusion from the matrix into the whiskers (or the reverse) may be critical. This subject has not received adequate attention.

MAGNETIC AND ELECTRICAL PROPERTIES

Fibers of several ferromagnetic materials have been prepared and their magnetic properties studied. The magnetic and electrical properties of iron whiskers have received particular attention. These investigations [14] have furnished important contributions to the properties of solids.

SURFACE PROPERTIES

Whiskers are small crystals of a high degree of perfection. Their surfaces, when examined in detail by both optical and electron microscopy, reveal dislocations, growth steps, localized defects due to impurities and voids, surface corrosion, oxidation, and surface nuclei. The physiochemical conditions and behavior at interfaces between whisker surfaces and liquid, or solid matrix materials in contact with them, do not appear to have been extensively investigated.

POLYCRYSTALLINE FIBERS

Filaments of polycrystalline inorganic, non-metallic materials have been prepared from ZrO_2, $ZrO_2 \cdot SiO_2$, Al_2O^3 and boron, as well as from various carbides, silicides, beryllides, nitrides, and other oxides. One method of preparing polycrystalline fibers is based on the employment of colloidal suspensions or solutions of decomposable salts. [36] The filaments produced by this method do not resemble whiskers; they have rectangular cross-sections and are not single crystals.

The process commonly employed for making polycrystalline filaments is that of incorporating the powdered inorganic materials into an aqueous or organic plasticizing agent and binder. This system is made into filaments by respectively drawing, pulling, or extruding, followed by baking to remove the binder, and finally, sintering. The processes and characteristics of polycrystalline filaments were recently discussed in a condensed review. [39] Much attention has been given to boron prepared by vapor deposition on refractory wire. Boron fibers on a tungsten substrate are reported to have E-values of 55 million psi, and tensile strengths (as formed) of 400,000 psi. After removal of the tungsten (boride) wire substrate, the strength reached 850,000 psi. Three routes are currently under investigation for preparation of polycrystalline filaments—vapor deposition, electro-deposition, and vacuum deposition on such substrates as tungsten, stainless steel, molybdenum, and vitreous silica. Other processes of potentially greater efficiency are based on passing aqueous suspensions through an orifice, followed by stretching, drying, and sintering.

METAL WIRES

Metal wires may be produced by various techniques, including spinning, slitting, and chemical, but these tend to yield non-uniform products of relatively short lengths. Those of interest here usually are prepared by extrusion or drawing methods. Wires of 6-mil diameter have tensile strengths at room temperature varying from about 600,000 psi to about 60,000 psi, depending upon the composition.

General Summary of Composites

CONCEPT AND THEORY OF FIBER-REINFORCED COMPOSITES

The requirements for high-strength components, particularly for high- and ultra-high temperature service are in excess of those that can be met with conventional materials. The good oxidation and corrosion resistance of ceramics, together with their high strength, high modulus of elasticity, and low density, seems to comply with the general requirements sought in advanced new materials. Physical mixtures of metals and ceramics have been tried in efforts to prepare composites with the desired mechanical and physical attributes, resulting in cermets and dispersion-hardened systems. The third system, fiber reinforcement, seems to offer exceptional promise, which NASA realized at an early date. In 1959 and 1960, reports were issued by McDanels et al.[38,39]

An excellent state-of-the-art survey of fiber-reinforced metallic composites was recently prepared and issued by J. W. Weeton.[40] A good paper on fiber-metal composites was given at the Twelfth Sagamore Army Materials Conference, August 1965, by Weeton and Signorelli.[41]

The potential advantages of fiber-strengthening are summarized below:

(1) The fibers carry the major portion of the load, and the matrix needs only to transfer the imposed tensile stress from fiber to fiber. Under favorable circumstances, only a small shear stress in the matrix is required for this transfer, allowing metal-fiber composites to operate at temperatures much closer to the melting points of matrix metals than for non-reinforced conventional materials. The fibers, in effect, reduce stress in the metal matrix members, resulting in retentions of strength in the composites at temperatures far above those allowable in the metal alone. This effect is not characteristic of solution-, precipitation-, or dispersion-hardening.

(2) By employing oxide or non-metallic whiskers as reinforcements which themselves approach theoretical strength, very high-ultimate strength in composites is possible. An additional advantage may be derived by preferential alignment or orientation of the fibers.

(3) Matrix materials can be metallic, ceramic, or organic (plastic), with an equally wide choice for the fiber-reinforced component.

(4) So far, it has been shown that fatigue occurs in whiskers, but whiskers are not so sensitive to surface damage as are conventional bulk materials; sapphire whiskers can be chopped and milled without loss of mechanical strength.

(5) Through the use of fiber components as a major constituent, it is expected that non-brittle ceramics are possible.[42] The incorporation of fibers into ceramics can add toughness and damage the failure mode, lessening brittle fracture.

(6) Very small chopped fibers may be incorporated into glass fibers to increase the modulus of elasticity.

(7) Fracture toughness and brittleness can be controlled to suit the requirements. Brittleness, characteristic of dispersed phase systems and cermets, can be modified.

(8) Where low-density fibers are used, favorable strength-to-weight ratios can be obtained.

At this stage in the development of fiber-reinforced composites, several disadvantages remain. These may be generalized as follows:

(1) Whiskers and ceramic fibers are still very expensive.

(2) The technology concerning the dispersion, wetting, and bonding of non-metallic fibers with metallic matrices, though of primary importance, has not been developed.

(3) Conventional methods for joining and processing fiber-reinforced composites are not applicable.

(4) Fiber lengths and the bond to the matrix should be adequate to take advantage of mechanical properties of the fiber component. Fibers need not be long to insure a relatively small shear stress at the fiber-matrix interface, but it is required that there be proper balance between fiber and matrix so the matrix can transfer most of the load to the fibers, fiber by fiber.

(5) There are problems with stress concentration at the ends of the fibers, which may have a bearing on stress initiation and propagation.

(6) Critical problems in the preparation of composites still exist; namely, the necessity for uniform distribution of the reinforcement fibers, the requirement of a strong bond between fiber and matrix, and the prevention of contamination of the fibers by the matrix, or the matrix by the fibers.

(7) Reinforcement by discontinuous fibers' functions through the mechanism of the transfer of loads from the matrix to the fiber. This ability depends upon the length-to-diameter ratio of the fibers, adequate fiber-to-matrix bond, and favorable values of modulus of elasticity. The required length-to-diameter ratio (aspect ratio) depends upon the ratio of the elastic modulus of the fiber to that of the matrix. Examples of these ratios for ceramics, metals, and plastics are as follows:

	Type of Matrix		
	Ceramics	Metals	Plastics
Ratio of elastic modulus of fiber to matrix	2:1	5:1	100:1
Optimum aspect ratio $\left(\dfrac{L}{D}\right)$	10–20:1	20–50:1	30–100:1

A review of fiber reinforced theory was recently published by Kelly and Davies.[3] McDanels et al.[38,39] have discussed the tensile strength of metals reinforced with continuous unidirectional fibers.

Fracture toughness apparently has not been given extensive theoretical treatment, but Cottrell[43] postulated a method for producing composites especially for fracture toughness. Using the relation $\sigma = \alpha\,E$, where σ is yield or fracture stress and E is Young's modulus of elasticity, from atomic displacement it is expected that $\alpha \simeq 0.1$ for nearly all solids.

Boron Carbide Whiskers

CONSIDERATION OF GROWTH METHODS

Three methods of growing B_4C whiskers have been investigated for NASA.[44-47] These are (a) the pure vapor method, (b) a modification of the pure vapor method, utilizing a carrier gas, and (c) the chemical method.

PURE VAPOR METHOD

By this method, boron carbide powder was heated to about 3500° F, converting some of the powder to vapors. The rising vapors condensed on cooler graphite surfaces, producing acicular crystals of small cross-section, called *whiskers*. Original preparations of B_4C whiskers utilized a large furnace into which one small whisker-growing unit was placed.[44] This configuration consisted, in part, of a graphite cup of 1-inch inside diameter by $\frac{3}{8}$-inch deep, filled with 325 mesh B_4C powder and set on a pedestal to raise the cup and its contents 2 inches into the hot zone of a large furnace. A long graphite tube with a conical top-section was placed over the container of B_4C powder to serve the combined functions of a stack and a deposition mandrel. This was 3 inches in diameter by 9 inches in total height. The top $5\frac{1}{4}$ inches was conical, being reduced over its length from 3 inches to $1\frac{3}{4}$ inches at its upper terminus. This stack-mandrel assembly rested on the floor or hearth-plate in the furnace and extended through the hot zone and out of it at its upper portions, thus providing a gradient of decreasing temperature from the position of the boron carbide powder to the $1\frac{3}{4}$ inch terminus.

With this arrangement, when the furnace was operated at 3450° F, the temperature in the bottom 1-inch of the chimney section was 3100° F, providing a cooler area for the disposition of the B_4C vapor (evaporated at 3450° F). During a typical run, the furnace pressure was 75 microns;
the temperature of the growth area was critical. A 50-degree change in furnace temperature appreciably altered the character and yield of the B_4C product.

The initial arrangements resulted in low yields of micron-length B_4C crystals. After successive changes, the final arrangement resulted in heavy growths of long whiskers. It was learned that the rising vapors were mainly concentrated in a narrow conical zone about the central axis of the system. A more effective system was developed, as illustrated schematically in figure 1.

PURE VAPOR WITH CARRIER GAS

A number of carrier-gas trails resulted in a combination that would produce optimum yields. Best results were obtained with argon at about 60 to 75 microns of vacuum.

CHEMICAL METHOD

The chemical method depends on the production of boron carbide *in situ* from a gas phase reaction, such as:

$$4BCl_3 + CH_4 + 4H_4 \rightarrow B_4C \times 12HCl$$
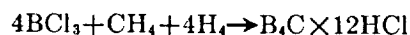
This method was not so successful as the pure vapor method.

RECOMMENDED GROWTH METHOD

PURE VAPOR METHOD

Presently, the pure vapor method is recommended to be most effective. With this method, a charge of B_4C powder is heated in a "lazy susan" type tray at 3500° F in 50 to 75 microns of argon. Whisker growth takes place on a graphite mandrel located above the evaporating zone, as illustrated in figure 1.
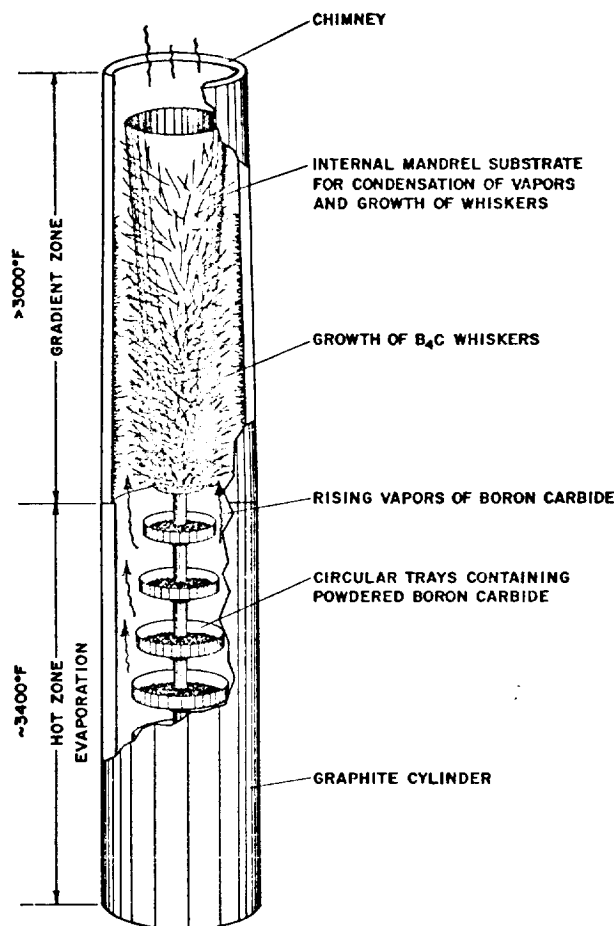
CHIMNEY

INTERNAL MANDREL SUBSTRATE
FOR CONDENSATION OF VAPORS
AND GROWTH OF WHISKERS

GROWTH OF B₄C WHISKERS

RISING VAPORS OF BORON CARBIDE

CIRCULAR TRAYS CONTAINING
POWDERED BORON CARBIDE

GRAPHITE CYLINDER

GRADIENT ZONE

>3000°F

HOT ZONE
EVAPORATION

~3400°F

FIGURE 1.—Unit for growing boron carbide whiskers at operating atmosphere—50–75 microns of argon.

DESCRIPTION OF EQUIPMENT

Growth is carried out in a large graphite-resistance furnace. Although whiskers develop in small laboratory furnaces, production-type runs require large furnaces. Gatti et al.[44,45] used a furnace having a 54-inch diameter and a 10-inch-long hot zone, capable of reaching 4000° F, although for preparing B₄C whiskers, it was operated at 3500° F in 50 to 75 microns of argon. The important point is that a graphite furnace, at least 5 inches long, having a hot zone over a large area and capable of operating at 3500° F in 50 microns of vacuum is required.

Whisker growth can then be carried out by placing numerous units, of the type illustrated in figure 1, on the furnace hearth. For example, a large furnace with a 60-inch diameter would have about 2800 square inches of setting space. If the unit shown in figure 1 were 2 inches in outside diameter, almost 700 of the units could be set in the furnace. If each lazy susan contained 180 square centimeters for boron carbide exposure, 700 such units would expose 126,000 square centimeters, or almost 20,000 square inches. Although there is a wide choice in furnace size and design, in this particular presentation no specific size and design is recommended.

Gatti et al.[44] used several experimental lazy susans. The larger one, with a total tray area of 180 square centimeters, had 15 trays on the spindle. The bottom tray was 1¼ inches in diameter, and each succeeding tray was smaller so as to grade into a top tray of about ½ inch in diameter. The number of trays and their sizes should be selected for maximum effectivity in the furnace used.

The same quality of whiskers could be grown either in a vertical or horizontal furnace. Even a small unit, with a tube diameter of 2½ inches, and holding only one of the whisker-making units of the type shown in figure 1 (or its equivalent), is effective.

The geometry of the crystal growth area is important, since geometric conditions can affect either the chemical gradient of the vapor available for deposition or the supersaturation of the vapor itself. It is believed that vapor species present in the deposition area are under molecular flow conditions due to the low operating pressure. Thus, the deposition was derived from a hollow cylinder-like volume of active vapor, which was about 1½ inches in outside diameter (the I.D. of the mandrel itself) by about ⅜ inch in depth, as evidenced by whisker lengths produced. The core volume of vapor (about 1 inch in diameter) was, in early work, being pumped out and wasted. Subsequently, an additional deposition surface was attached to the top of the lazy susan tray arrangement in order to utilize this central core of vapor. (This deposition surface is illustrated as the inverted cone in the top section of figure 1.) The mandrel is purposely hollow to minimize effects on temperature gradients. The dimensions of the inverted conical mandrel should be established by experiment to yield optimum performance in the equipment selected.

Internal mandrel lengths of 5, 6, and 7 inches were tried with no improvement over the original 4-inch mandrel, which probably should have a smaller small-diameter cross-section than is illustrated. The conical shape, although recommended, has not been tried. Successful operations have been conducted[49] in which a half-inch-diameter graphite cylinder, 4 inches long, was mounted where the inverted cone is shown in figure 1.

FURNACE CONDITIONS

The operating temperature depends somewhat on the geometry of the configuration setting. In general, optimum operating conditions are 5-hour duration heats with a temperature of 3500°F in the evaporation zone, and approximately 3150°F in the whisker-deposition zone, which may grade down to 2900°F. Typically, the furnace is operated at 50 microns pressure of argon. The effect of temperature on the growth process is critical, and a 50°F change in temperature can appreciably alter the length and population density of the boron carbide whisker product. The operating temperature is higher for small furnaces than for large furnaces. The temperatures mentioned here are subject to minor revisions, depending on design and other criteria.

FURNACE CHARGE

The lazy susan trays are filled with B_4C powder, 325 mesh grade. The use of boron and boron plus carbon has not been effective for the production of B_4C whiskers, for reasons not ascertained. The presence of vanadium, molybdenum, or niobium in minor amounts in the charge is essential for the growth of B_4C whiskers. These impurities promote both the yield and the rate of growth of B_4C crystals. Experience on which these conclusions are based was obtained with one weight percent of the additive. Vanadium was more effective than molybdenum or niobium.

During a run, B_4C powder tends to be depleted of impurities, including the "catalysts." Exhausted powder was not effective for the production of B_4C whiskers. The growth of whiskers obtained by the addition of vanadium to exhausted B_4C powder was equal to the best obtained with fresh powder. Without additions of the catalyst, five or six runs with the same powder were sufficient to reduce production to zero.

CONSTITUTION OF THE VAPOR

The vaporization of B_4C at various temperatures has been studied by several investigators, including Robins and Giles.[48] Their data indicated that B_4C was not vaporized directly, but was transmitted as elemental boron along with intermediate species of BC_2 and B_2C. The intermediate phases might amount to 4 percent of the total vapor, but the bulk of the vapor consisted of elemental boron. However, when boron was substituted for B_4C in the process for the starting reagent, no whiskers of B_4C were produced, even when 1 percent of vanadium was added. After the graphite trays charged with elemental boron were heated for 5 hours at 3500°F, the boron was partly converted to B_4C, which eventually produced some boron carbide whiskers on reheat runs.

PRINCIPAL FACTORS

Yields of B_4C whiskers can be produced by the evaporation from B_4C followed by subsequent condensation of the vapors, as follows:

(1) The trays with their charge of boron carbide powder should be heated at about 3500°F, although this may vary somewhat with furnace design. The hot zone temperature is critical, and a 50°F change in operating temperature can appreciably alter the size, population, and yield of B_4C whiskers.

(2) It is recommended that the furnace be operated at 50 microns of vacuum, and the gas present be argon plus boron-bearing vapors.

(3) The recommended mandrel should be located above the uniform hot zone where the B_4C powder is placed, and the hot end of the condensation mandrel should be maintained at 3150°F. Under some conditions of configuration, these temperatures might be 100°F lower.

(5) An effective arrangement consists of a

stack of graphite trays filled with B₄C to be vaporized, above which is located a graphite mandrel as a substrate for crystal growth and the assembly set in a tapered graphite stack. For production, many such units may be set on the hearth of one large furnace.

(6) The starting powder in the evaporation trays must be B₄C; boron will not work. The use of 1 percent of vanadium added to the B₄C powder greatly increases the yield of boron carbide whiskers.

(7) Overheating causes whiskers to develop surface growths which tend to reduce their mechanical strength.

(8) The B₄C reagent becomes progressively less effective for producing whiskers after each run, but can be rejuvenated by minor additions of vanadium or, to a lesser degree, by molybdenum and columbium. Additions of 1 percent of the contaminants have been successful.

(9) The geometry of the whisker growth area is of primary importance, since geometric conditions can affect the chemical gradient, the temperature gradient, and the saturation of the vapor itself. The geometry in the deposition zone can greatly influence yields of whiskers.

MORPHOLOGY

The morphology of B₄C whiskers was treated in detail by Gatti et al.,[47] where the discussion deals with whiskers thicker than 1000 Angstrom units. High magnification, 875 X and above, showed the presence of surface features. The most common topographical feature was a series of flat-topped elevations or flat-bottomed depressions with boundaries observed to have definite angular relationships (60° to 120°) to each other, and to the whisker axis (0°, 60°, or 120°). The general appearance was one of a metropolitan skyline in which the buildings and walls were 60° to 120° to one another. Another

common feature was that relatively long lines or flutes were directed parallel to the whisker axis, consisting of step-like formations. The risers formed steps normal to the major whisker surface.

With the exception of their tips, the whiskers are single crystals over their entire length, with their major axes parallel to (h00) crystallographic direction. The stacking faults and morphological surface configuration can serve as grips and anchors in composite structures.

Nucleation occurs only on the substrate, not on whisker surfaces, and is probably greatly influenced by the nature of the substrate. This indicates that the population density and orientation of the whiskers may be controlled through the choice and selection of substrate materials.

Growth in the direction of the major axis terminates when the whisker reaches a level in its ambient growth environment where the degree of vapor supersaturation will not support regular or periodic growth. Therefore, the nature of the vapor phase in terms of its concentration in the vicinity of the growing whisker influences its ultimate length. Longer whiskers can be grown by decreasing the concentration gradient of the vapor in the direction of whisker growth. This may be done by carefully controlling the temperature gradient in this region through the introduction of properly shaped (finned) mandrels, and so forth.

PROPERTIES

The mechanical properties of B₄C whiskers have not yet been evaluated in detail. Thus far, from a total of 20 tests,[44] tensile values have varied from a low of 179,000 psi to a high of 965,000 psi, with an average value of 400,000 psi. Values near 65 million psi have been determined for Young's modulus. The influence of fiber diameter, crystallographic orientation, and temperature on stength, has not been fully ascertained. It is expected that mechanical properties will resemble those for sapphire and silicon carbide.

Boron Filaments

METHOD OF PREPARATION

Under NASA contract, experimental boron filaments were prepared by Witucki,[49] where a continuous laboratory process similar to that described by Talley [50] was used.

A $\frac{1}{2}$-mil tungsten wire was the substrate on which boron was deposited by vapor decomposition. In this process, the wire was heated in a chamber containing flowing hydrogen in order to clean the wire. Appropriate mercury seals were provided at each end of the tube. The mercury also provided electrical contacts to the wire so it could be heated to about 1200° C (2200° F). From this tube, the wire passed directly into a similar chamber where the boron deposition was accomplished. In this chamber, the wire was heated to a temperature range of from 1000° C (1832° F) to 1200° C (2200° F). Through this chamber was passed a mixture of BBr_3 and H_2 which reacted at the heated tungsten surface and deposited amorphous boron. At temperatures in excess of 1200° C, the amorphous boron begins to crystallize with a resultant decrease in strength.

Boron deposition is the result of surface reactions which do not occur at the same rate at all points on the surface, resulting in fibers of irregular surfaces. Subsequent improvements in technique that permit longer reaction times and include automatic recycling of unreacted boron bromide have minimized these irregularities.

PROPERTIES

Strength-to-weight ratios for boron filaments are very high. The properties of particular interest are the high melting temperature, 2040° C; high modulus of elasticity, 55×10^6 psi; low density, 2.35 g/cc; and considerable retention of strength at temperatures to 1000° C.

Large variations have been observed in tensile strengths of individual filaments. Values have been observed to vary from 25,000 psi, for filaments with flaws, up to 300,000 psi. Some fibers produced under optimum conditions have been observed to have higher strengths. Those examined had diameters of 1.8 to 2.0 mils. It appeared that the filaments deposited on tungsten wires are characteristically under high residual stress and frequently exhibit spontaneous crackup.

Characteristic surface appearances are shown in figure 2(a), (b), and (c). Figure 2(b) shows the characteristic nodular surface as well. Cracks in the filaments are sometimes visible, as shown in the sketch of the magnified cross-section in figure 2(c).
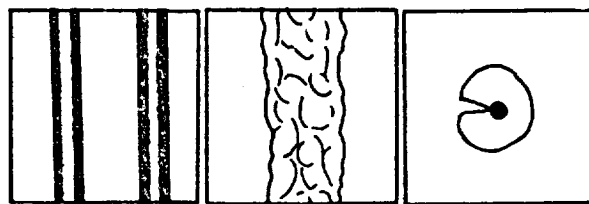

FIGURE 2.—Boron filaments, 3.1 mil diameter—(left) about 50X; (center) about 320X; (right) showing etched crack, end view, about 150X.

Refractory Ceramic Fibers

CLASSIFICATION OF FIBERS

Gates and Lent[51] classified the materials covered here as glass. Technically, the materials as prepared were undoubtedly glass, particularly because of the rapidity with which they were quenched. But glass technologists, upon examination of the compositions involved, would not expect them to form stable glasses. They would expect the products, as made, to be glassy but to crystallize readily into polycrystalline forms when heated to moderate temperatures, say in excess of 1800° F.

The term "refractory glass" is misleading—the compositions described here certainly are refractory as compared to conventional glasses, but probably cease to be glass soon after the first time the fibered products are heated at moderate temperatures (in the general range of 2000° F). Characteristically, glass, being a super-cooled liquid, will invariably soften when heated at temperatures in the lower red-heat ranges. All except the most stable glasses crystallize and cease to be glass when heated moderately above the softening temperatures; some glasses crystallize before reaching a glass-softening point.

In the products described here, advantage is taken of their relatively high viscosity at higher temperatures, which makes it possible to "fiberize" the materials while they are in a viscous state during initial cooling. Subsequently, when being used for high-temperature applications, the fibers crystallize into refractory polycrystalline products that do not have the low-temperature limitations characteristic of conventional glass.

PURPOSE AND COMPOSITIONS

In the aerospace industry, there has been an increasing need for high-temperature fibrous materials. Glass fibers are of relatively low manufacturing cost. Materials of interest that can be fiberized like glass, but that in use behave like refractory oxides instead of glass, are shown in table III. Characteristically, the compositions are exceptionally low in SiO_2 and high in Al_2O_3, MgO, or ZrO_2.

FIBER FORMING

Batch materials were placed in appropriate refractory containers (usually tungsten) and preheated in excess of 3200° F (1750° C) with oxygenacetylene flames. Auxiliary heating was accomplished with immersed tungsten electrodes, without the gas flames. An arc was struck between tungsten electrodes which were covered with glass batch. The electrodes were slowly separated so that the current continued to flow through the melt between the electrodes until the container was one-third filled with the liquid products at a desired temperature.

When desired, it was possible to discharge a continuous stream of molten glass. A water-cooled, welded, stainless steel hearth plate with an orifice insert of an oxidation-resistant Ni-Cr-Fe alloy was used. Fiberizing was done through a high-pressure attenuating nozzle, schematically illustrated in figure 3. A typical fiberizing run took 10 seconds to blast 50 grams of glass. While diameters of fiber varied, they were generally 15 to 25 microns. A typical yield would be 20 percent of fiber and 80 percent of "shot." The average fiber length was about 1.5 inches. Additional yield details are given in table III.

PROPERTIES

Fiber diameters depend upon a number of factors, and ranged from as low as 6 microns to as great as 50 microns. Fiber lengths and other details are given in table III. Tensile strengths

TABLE III.—*Selected Fiber Compositions*

Composition Number	SiO₂	Al₂O	MgO	ZrO₂	PbO	ZnO	Sb₂O₃	Sa₂O₃	CeO₂	Y₂O₃	P₂O₅	CaF₂	V₂O₅	Fiber Yield, gm per 50 Blasts	Fiber Fusion Temp., °C	Comments
R45	36.00	48.00	16.00											6.6	1475	Fine long fibers, low viscosity
R58	25.00	56.00	19.00											3.0	1495	Extremely fine short fibers
R59	35.50	30.50	9.50	24.50										5.8	1450	Very fine short fibers, high viscosity
R66	42.75	15.25	4.75	37.25										1.4	1500	2–3 inch fine fibers
R74	50.00	22.50	7.50	20.00										8.6	1450	Fairly fine long fibers, easy to fiberize
R76	60.00	7.50	2.50	30.00										3.2	1605	1–6 inch fine fibers, difficult to fiberize
R79	20.00	45.00	15.00	20.00										3.0	1550	4–6 inch fine fibers
R86	45.00	45.00			10.00									1.2	1680	Short fibers, very high viscosity
R87	40.00			40.00		20.00								2.0	1680	Medium fibers, very high viscosity
R89	35.00	32.50				32.50								1.5	1620	Medium fibers, good quality
R91	25.00	62.50	12.50											2.0	1620	2–4 inch fine fibers
R99	50.00	27.00	3.00	20.00										7.0	1580	Long, flexible fine fibers
R108	17.90	35.70				35.70	10.70							1.3	1830	1–2 inch very fine fibers
R110	18.50	37.00				37.00		7.50						1.2	1830	½–2 inch very fine fibers
R112	17.90	35.70				35.70			10.70					1.4	1750	½–1 inch fine fibers
R113	18.50	37.00				37.00				7.50				1.6	1750	1–2 inch fine, uniform fibers
R117	54.50	6.83	2.27	27.20							9.20			1.0	1505	1–6 inch glassy fibers
R119	60.00	10.00		30.00										3.4	1575	Medium texture fibers, viscosity lower than R–76
R123	58.20	7.28	2.42	29.20				2.90						2.2	1575	1–3 inch fine textured fibers, pink
R132	45.00	40.00									15.00			1.2	1790	1–3 inch fine fibers
R141		57.00										43.00		1.4	1530	Low viscosity melt, 1–2 inch fine fibers
R145	57.70	7.20	2.40	28.70									4.00	1.0	1485	Fine short dark gray fibers
R147	56.96	7.08	2.36	28.60					5.00					1.8	1500	Somewhat viscous melt short, fine fibers
R149	24.60	55.40										20.00		2.4	1500	Low viscosity, high surface tension, 2–3 inch fibers
R150	21.20	43.80				25.00						10.00		2.4	1520	Low viscosity, high surface tension, 2–3 inch fibers

•were measured for selected fibers. Typical mean values at room temperature were about 200,000 psi, with individual readings ranging from 500,000 to about 50,000 psi. Filaments of composition R-141 had a mean tensile strength value of 295,000 psi. No data are available on fibers after having been heated. The softening temperatures of various fibers are also shown in table III.

These products seem best suited for insulation, felting, and applications other than reinforcement of metals intended for sustained high-temperature components.
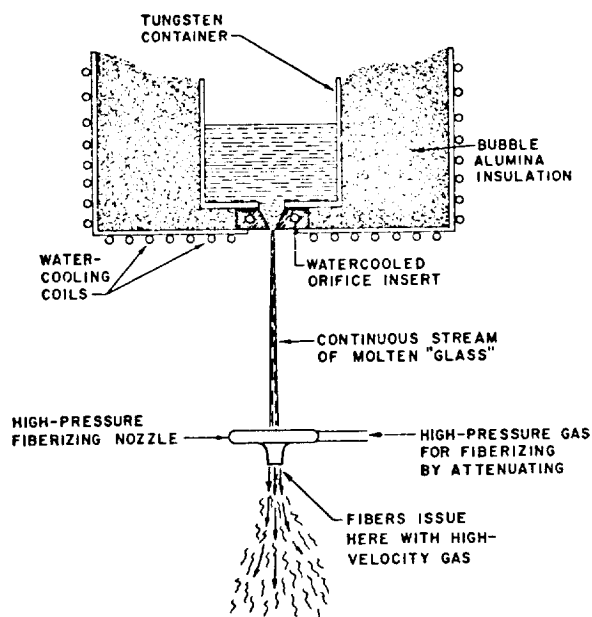
FIGURE 3.—Arrangement for fiberizing refractory glasses (heating elements not shown).

Metal-Fiber-Reinforced Metallic Composites

COPPER REINFORCED WITH TUNGSTEN FIBER 52-55

FIBERS

Commercially pure tungsten wires, 0.005 inch in diameter, were given a heat treatment similar to that required for the molten copper infiltration process (1 hour at 2200° F in vacuum) to ascertain what, if any, damage would be done to the tungsten filaments by the heat treatment. The tensile strength was consistently 330,000 psi after this annealing treatment, compared to a prior 390,000 psi. The only observed change in microstructure was in the longitudinal view, with none detected in cross-section views.

MATRIX MATERIALS

Copper with various alloying elements was used for matrices, shown in table IV.

SPECIMEN FABRICATION

The products obtained were tungsten fibers bound by the matrices shown in table IV. The tungsten fibers were aligned to be parallel to and of the same length as the long axis of the specimen.

The first step in the fabrication was to clean the 4-inch-long tungsten filaments with hot concentrated sodium hydroxide, followed by rinsing in distilled water, then with a boiling solution of ammonia in water and distilled water, in that order. The wires were inserted into a closed-end silica or ceramic tube to yield 65 to 80 volume percent of fibers, with a slug of the matrix metal in the bottom. The entire assembly was then held for 1 hour at an appropriate temperature in a resistance-heated vacuum furnace, resulting in tensile specimens illustrated in figure 4.
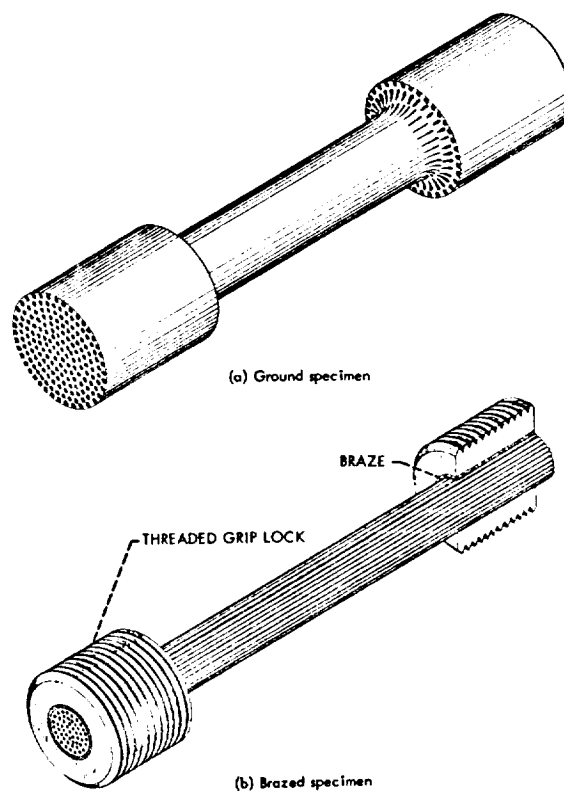

(a) Ground specimen

(b) Brazed specimen

FIGURE 4.—Ground tensile and brazed tensile specimens, showing relation of reinforcing fiber to specimen configuration.

TENSILE STRENGTH

Using pure copper as a matrix and aligned tungsten fibers, McDanels et al.[39] found tensile strength values to agree reasonably well with theoretical values. The fibers were 0.003, 0.005, and 0.007 inch in diameter. The strength of the composite depends upon whether the copper matrix or the tungsten fibers are the main constituent carrying the load. When tungsten

TABLE IV.—*Room Temperature Tensile Properties of Copper-Alloy, Tungsten Fiber Composites*

Binder Material	Maximum Solubility of Alloying Element in Tungsten	Weight Percent of Alloying Element	Atomic Percent of Alloying Element	Specimen	Volume Percent Fiber	Tensile Strength psi	Reduction in area percent	Type of Fracture
Pure copper	Insoluable in tungsten	0	0	-------	65	225,700	-------	Ductile
				-------	70.2	238,000	-------	Ductile
				-------	75.4	249,800	-------	Ductile
Copper-nickel	0.3	5	5.4	1	79	246,600	34	Ductile
				2	78.4	250,000	37	Ductile
				3	76	218,900	32	Ductile
		10	10.9	4	74.1	131,700	Nil	Brittle
				5	75.5	108,800	Nil	Brittle
				6	79.5	51,300	Nil	Brittle
Copper-cobalt	0.3	1	1.1	7	77.3	219,400	-------	Semi-ductile
		5	5.4	8	76	213,200	1.5	Semi-ductile
				9	74.8	229,300	2.3	Ductile
				10	74.7	147,200	-------	Brittle
				11	74.9	172,100	-------	Brittle
Copper-aluminum	2.6	5	11.3	12	63.4	98,900	Nil	Brittle
				13	72.4	153,800	Nil	Semi-ductile
				14	76.1	154,500	Nil	Semi-ductile
		10	20.8	15	76.7	138,500	-------	Brittle
Copper-titanium	8	10	12.8	16	78.2	223,700	-------	Semi-ductile
				17	71.7	220,100	10	Semi-ductile
		25	30.7	18	76.3	186,700	-------	Brittle
Copper-zirconium	3	10	7.2	19	72.8	216,000	Nil	Brittle
				20	78.5	255,300		Ductile
				21	75.6	226,900		Semi-ductile
				22	64.7	172,600		Brittle
				23	64.3	195,700	Nil	Semi-ductile
		33	25.5	24	75.9	106,700	Nil	Brittle
Copper-chromium	Complete solid solubility (Miscibility gap)	1	1.2	25	78.7	223,500	7.4	Semi-ductile
				26	77.5	228,600	25.8	Ductile
				27	77.2	225,900	7.5	Semi-ductile
		2	2.4	28	76.4	241,700	16.4	Ductile
Copper-niobium	Complete solid solubility	1	0.6	29	75.4	237,100	20.6	Ductile
				30	75.1	223,100	24.7	Ductile

fibers carry the major load, the equation is:

$$P = \sigma_C A_C = \sigma_F A_F + \sigma_M{}^* A_M$$

where:

P = load carried by the composite

σ_C = tensile strength of the composite

A_C = cross-sectional area of composite ($= 1$)

σ_F = tensile strength of fiber

A_F = fraction of cross-sectional area of composite occupied by fiber

$\sigma_M{}^*$ = stress on copper matrix

A_M = fraction of cross-sectional area of composite occupied by matrix $[= (1 - A_F)]$

The stress, $\sigma_M{}^*$, is that for pure annealed copper at the final elongation of tungsten, 1.5 percent. This is only about 35 percent of the elongation of copper at failure—the point where tungsten, which carries the load, would fail. For situations where the load-carrying capacity of the matrix and fibers is about equal, the expression is:

$$\sigma_M A_M = \sigma_F A_F + \sigma_M{}^* A_M$$

Calculated tensile strengths of composites for various volume fractions of tungsten wire are linear, having an intercept at 100 percent tungsten equal to the fiber and an intercept at 100 percent copper (zero percent of fiber) equal to 8000 psi. The strengths of experimental composites fell close to, and along, the calculated curve.

It is customary to refer to the ratio of length

(a) Copper plus 5 percent nickel matrix.

(b) Copper plus 10 percent nickel matrix.

(c) Copper plus 1 and 5 percent cobalt matrix.

(d) Copper plus 5 and 10 percent aluminum matrix.

(e) Copper plus 10 and 25 percent titanium matrix.

(f) Copper plus 10 and 33 percent zirconium matrix.

(g) Copper plus 1 and 2 percent chromium matrix.
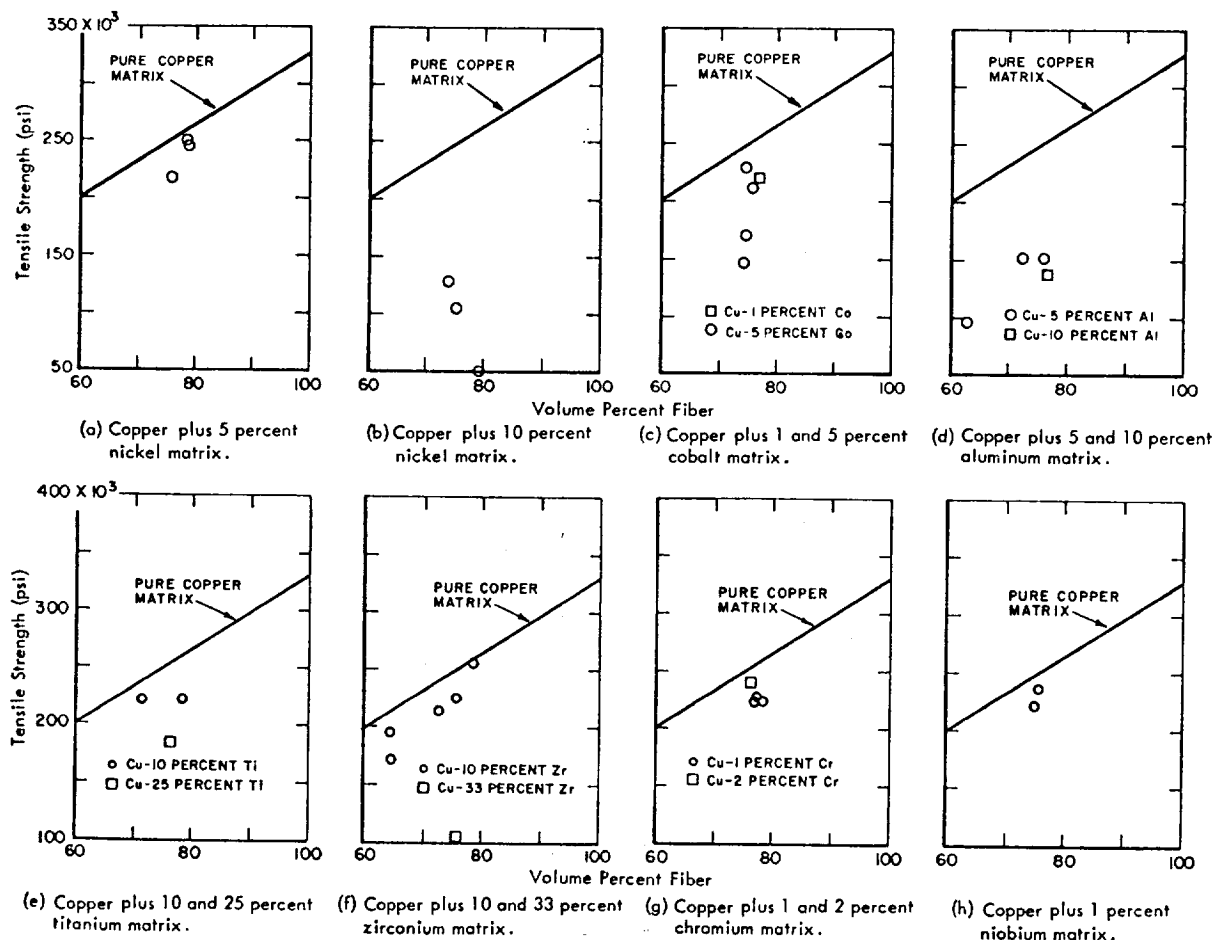
(h) Copper plus 1 percent niobium matrix.

FIGURE 5.—Strength-composition diagrams comparing copper-tungsten fiber composites to copper-alloy-tungsten fiber composites.
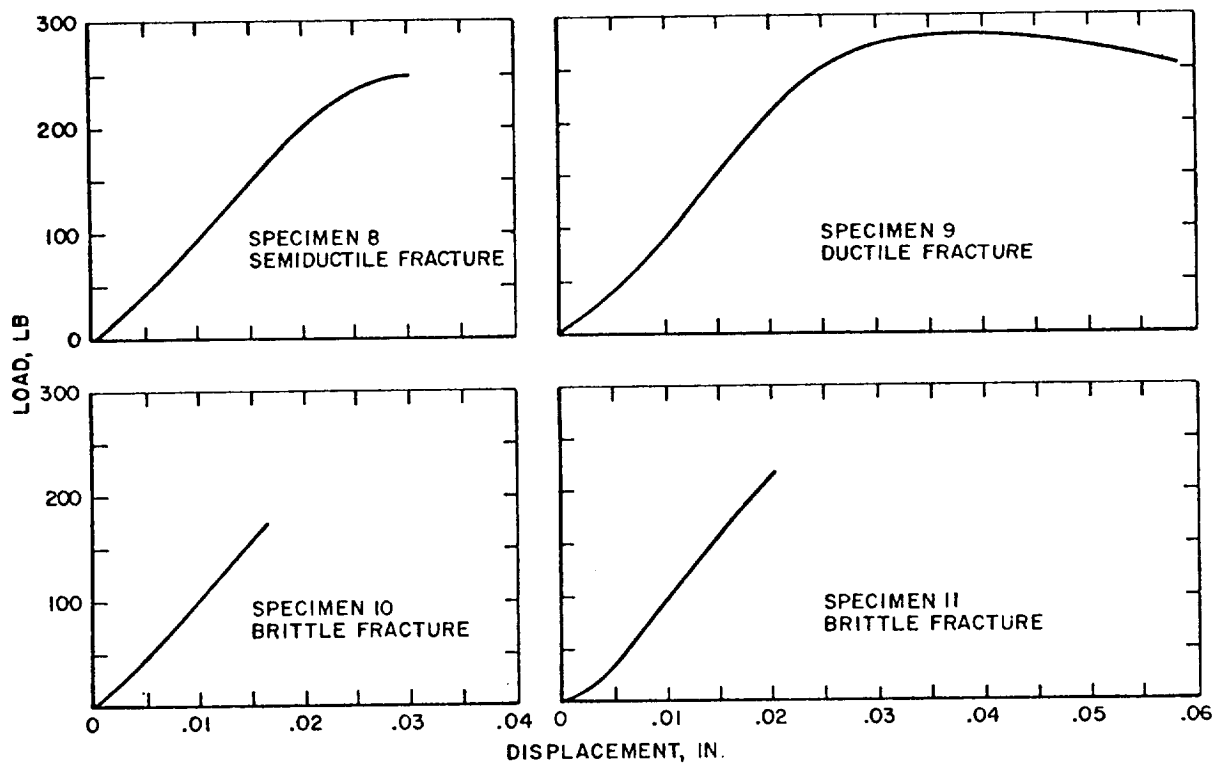
FIGURE 6.—Load as a function of displacement curves for tungsten-fiber-reinforced copper plus 5 percent cobalt composites.


FIGURE 7.—Pure copper matrix.

to diameter as the critical aspect ratio, which can be calculated by integrating the shear strength of the matrix around a fiber and equating this to the fiber strength. For the system of tungsten fiber in a copper matrix, a critical aspect ratio of 16:1 was calculated.

Tensile values of various compositions (shown in table IV) are diagramed in figure 5, where the solid, straight lines on each of the plots represent values that might be calculated for tensile strength of composites with 5-mil tungsten fiber and a pure copper matrix; the straight lines are for comparison and reference purposes.

Some composites, particularly those with copper matrices containing 5% Ni, 10% Ti, 10% Zr, 1 and 2% Cr, and 1% Cb, closely approximated tensile strengths obtained with the reference matrix of pure copper, while all others were substantially weaker.
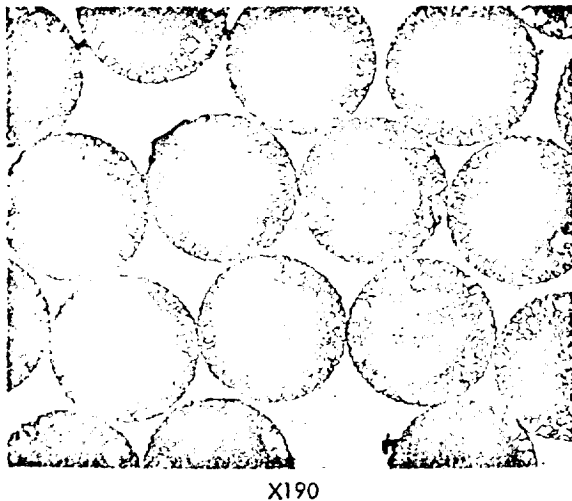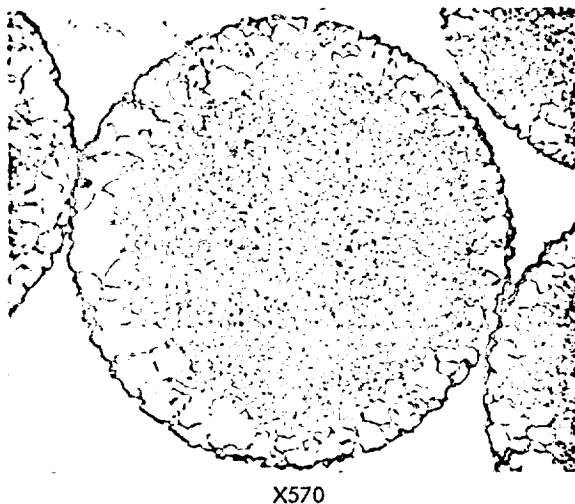
FRACTURE DUCTILITY

The reduction in area, which gives a qualitative indication of the degree of ductility, and a description of the type of fracture are given in table IV.

LOAD-DEFORMATION CURVES

Four types of load-deformation curves were obtained, as shown in figure 6. These curves represent elongation versus load, instead of unit values of stress and strain. The curves are representative of various types of fractures—brittle, semi-ductile, and ductile.

MICROSTRUCTURE

The microstructure of composities cut normal to the long axis of the fibers from a sample made with a pure copper matrix is shown in figure 7. There is no evidence of recrystallization in the tungsten fiber or of alloying at the three types of copper-tungsten interfaces observed.
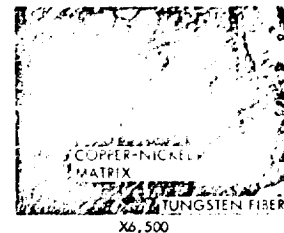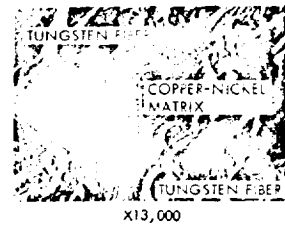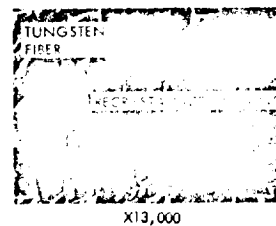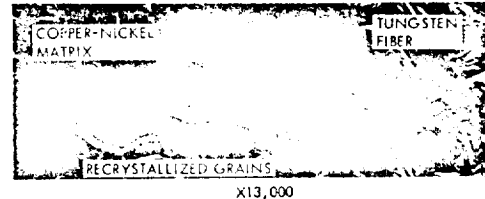

FIGURE 8.—Copper plus 10 percent nickel matrix—(left) diffusion-penetration reaction; (right) recrystallization of tungsten fiber.
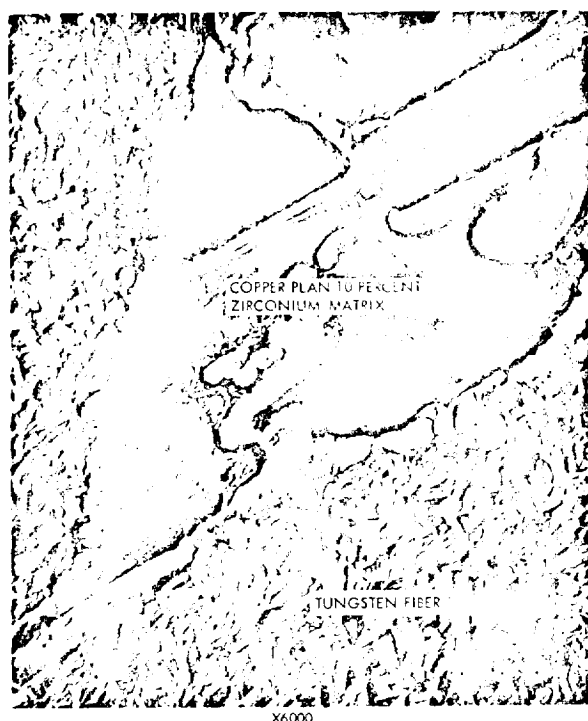
FIGURE 9.—Copper plus 10 percent zirconium tungsten-fiber composite.

(1) A diffusion-penetration reaction, together with recrystallization of the tungsten fiber at the interface of the matrix, is illustrated in figure 8. The recrystallization in the matrices differed among the compositions, but similar reactions were observed in matrices containing cobalt, aluminum, and 10 percent of nickel as additions to copper.

(2) A second type of interface, where a two-phase zone was formed, is shown in figures 9 and 10. Among the compositions investigated, Cu-Ti and Cu-Zr matrix materials had this type structure.

(3) Solid-solution reactions, occurring without recrystallization, resulted in still a third type of interface. Figure 11 is a photomicrograph of a sample section bonded with a Cu—1 percent Cr matrix.

The importance of physical and chemical compatibility between matrix and' aggregate (fiber) is clearly evident from the strength reduction data shown in table V. By comparing these results with figures 7 through 11, it is
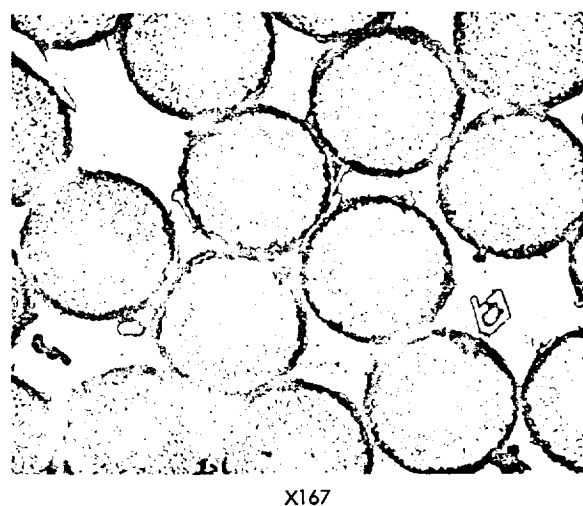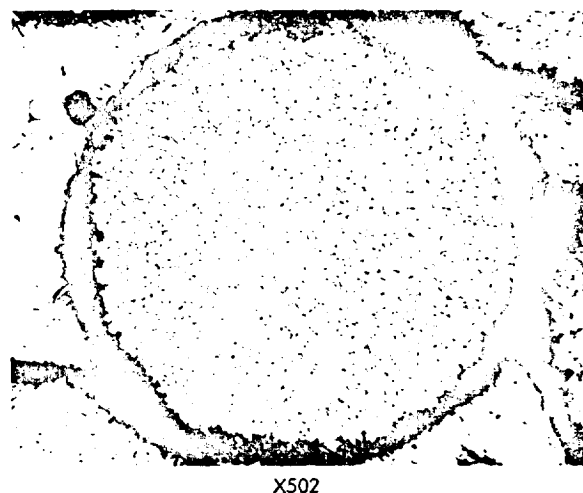

FIGURE 10.—Copper plus 25 percent titanium matrix.

evident that, for these cases, the most damaging type reaction at the interface was the diffusion-penetration accompanied by recrystallization. It is further evident that, in fiber-reinforced composites, deleterious interfacial reactions resulted in weakening instead of strength increases.

There is some correlation between depth of penetration at the interface with ductility of the composites, as shown in table VI. The greater the depth of penetration of the alloying element into the tungsten fibers, the lower the tensile strength and ductility of the composite. An equation relating to this follows:

TABLE V.—*Percent Reduction in Tensile Strength in Tungsten-Fiber-Reinforced Composites due to Alloying Agents in the Copper Matrix*

Matrix, Mole %	Reduction in Composites' Strength from Values Obtained with a Pure Copper Matrix	
	Decrease, psi	Percent Reduction
Cu—5 Ni	17,500	7
Cu—1 Nb	20,000	8
Cu—10 Zr	25,000	10
Cu—1 Cr	30,000	12
Cu—10 Ti	37,000	14
Cu—5 Co	62,000	24
Cu—25 Ti	68,000	27
Cu—5 Al	100,000	43
Cu—10 Al	117,000	46
Cu—33 Zr	143,000	57
Cu—10 Ni	160,000	62

$$\Delta\sigma_c = KA_f(2Pd_o - P^2)$$

Values of K and related data are given in table VI.

STRESS-STRAIN BEHAVIOR

Tungsten fibers in a copper matrix were selected as a model system because of their chemical, metallurgical, and physical stability in mutual contact. During fabrication, a good bond developed between tungsten and copper (using pure copper as the matrix), with no observed deleterious interdiffusion.

The behavior patterns for composites reinforced with either continuous or discontinuous tungsten fibers of 3-, 5-, and 7-mil diameter are indicated by the following values of tensile strength:

```
3-mil fiber_____331,000 psi
5-mil fiber_____327,000 psi
7-mil fiber_____290,000 psi
```

The average tensile strength of the annealed copper used for the matrix material was 27,800 psi. For composites of this type, the ultimate tensile strength is a linear function of the proportion of fiber in volume percent. These data are shown in figure 12(a), (b), and (c) for continuous reinforcement fibers of diameters of 3, 5, and 7 mils, respectively, and in 12(d) for discontinuous 5-mil diameter tungsten fiber. There is a definite trend for the elongation at
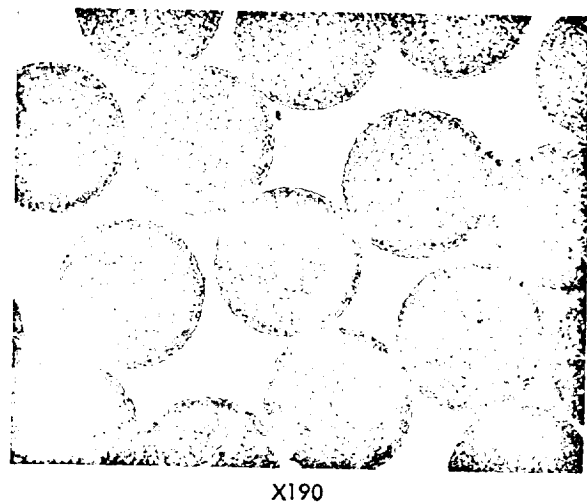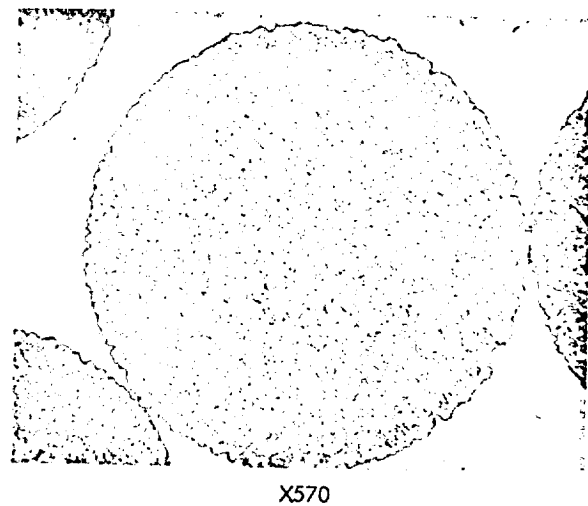

X570

X190

FIGURE 11.—Copper plus 1 percent chromium matrix.

failure to decrease with increased fiber content, as shown in figure 13.

Typical stress-strain curves for tungsten fiber, copper, and some composites comprised of these materials, are shown in figure 14. The composites reach their ultimate tensile strengths at about 1.4 percent of strain; the copper component develops plastic flow at very low strain; and the tungsten is elastic until it reaches about 0.4 percent of strain. The low-strain region is plotted on an expanded scale in figure 15, where it is shown that the elastic limit of copper is about 0.03 percent of strain, clearly indicating the influence of the
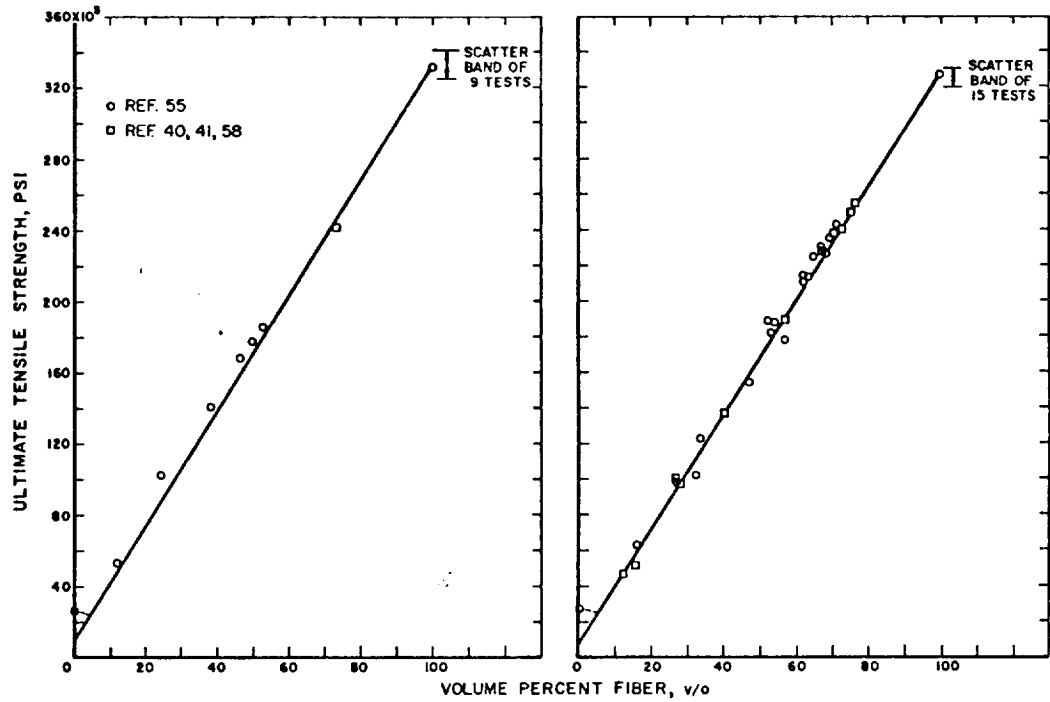
(a) Continuous reinforcement with 3-mil-diameter
    tungsten fibers.

(b) Continuous reinforcement with 5-mil-diameter
    tungsten fibers.
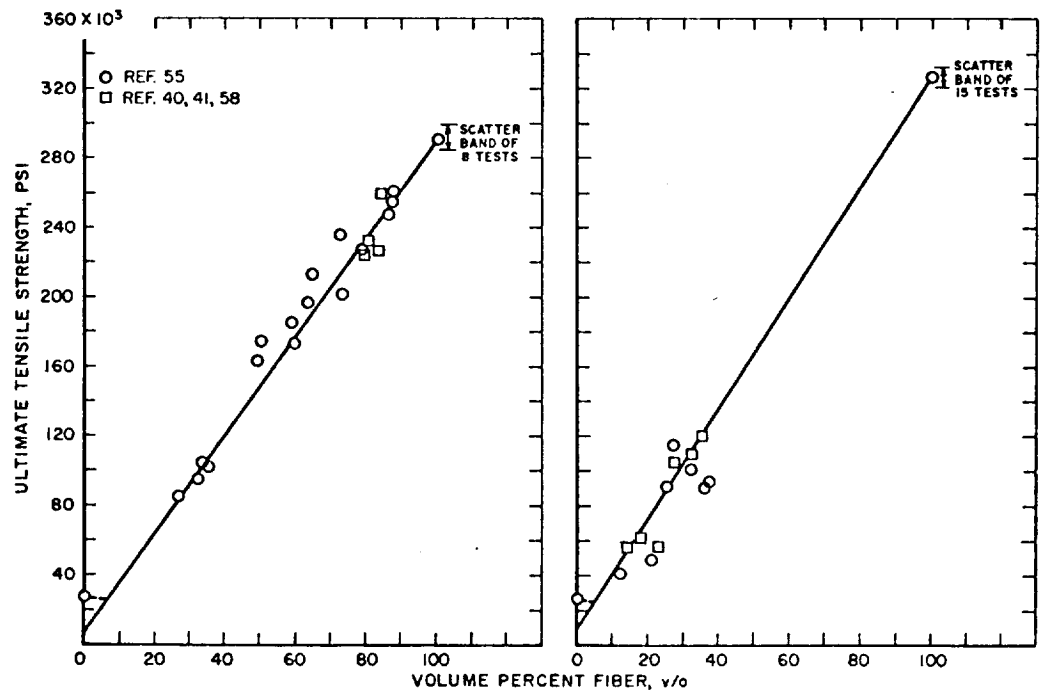
(c) Continuous reinforcement with 7-mil-diameter
    tungsten fibers.

(d) Discontinuous reinforcement with 5-mil-diameter
    tungsten fibers.

FIGURE 12.—Tensile strengths of tungsten-fiber-reinforced copper composites.

TABLE VI.—*Comparison of Ductility and Depth of Penetration with K*

Alloy	Speci-men	Type of Fracture	Change in Tensile Strength of Composite, $\Delta\sigma_c$, psi	Percent of Cross-section Occupied by Fiber, A_f	Twice the Depth of Depth of Penetration, P, in.	$K = \dfrac{\sigma_f - \sigma_P}{d_o^2}$ lb/in.^{4}
Cu—5% Ni	1	Ductile	18,400	79	0.000106	223×10^{-8}
	2	Ductile	10,000	78.4	0.000106	122
	3	Ductile	36,000	76	0.000106	452
Cu—10% Ni	4	Brittle	115,800	74.1	0.00087	195×10^{-8}
	5	Brittle	143,000	75.5	0.00158	143
	6	Brittle	214,000	79.5	0.00155	206
Cu—5% Co	8	Semi-ductile	42,000	76	0.00085	71×10^{-8}
	9	Ductile	21,000	74.8	0.00076	40
	10	Brittle	103,000	74.7	0.00168	99
	11	Brittle	78,000	74.9	0.00135	89
Cu—10% Ti	16	Semi-ductile	38,300	78.2	a 0.000104	476×10^{-8}
	17	Semi-ductile	38,000	71.7	0.000104	515
Cu—10% Zr	19	Brittle	26,000	72.8	a 0.000104	347×10^{-8}
	20	Ductile	5,000	78.5	0.000104	64
	21	Semi-ductile	23,000	75.6	0.000104	296
	22	Brittle	43,400	64.8	0.000104	645
	23	Semi-ductile	17,300	64.3	0.000104	262
Cu—1% Nb	29	Ductile	15,000	75.4	a 0.000104	193×10^{-8}
	30	Ductile	28,000	75.1	0.000104	362

Legend: $\Delta\sigma_c$ = difference in tensile strength between tungsten-fiber-copper composite and tungsten-fiber-copper alloy composite

A_f = area percent of fiber in cross-section of composite

σ_f = tensile strength of fiber

σ_p = tensile strength of alloyed zone of fiber

d_o = initial diameter of fiber

a = estimated value

fiber content. The slopes at low values of strain may be termed the region of initial modulus of elasticity, and the slopes above the break called the secondary modulus of elasticity.

The secondary modulus of elasticity of the tungsten-copper composites is a linear function of the volume percent of tungsten fiber, as shown in figure 16. Yield values of the composites are likewise a linear function of the volume percent of fiber, as shown in figure 17.

Upon application of tensile stress, four stages of deformation are recognized:

(1) During initial loading stages, both the matrix and the fiber (composite) deform
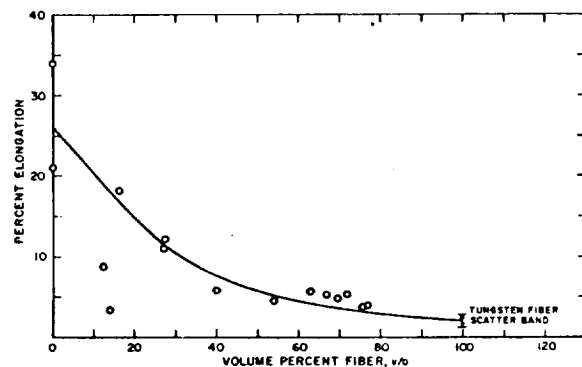
FIGURE 13.—Elongation at failure of composites reinforced with continuous 5-mil diameter tungsten fibers.
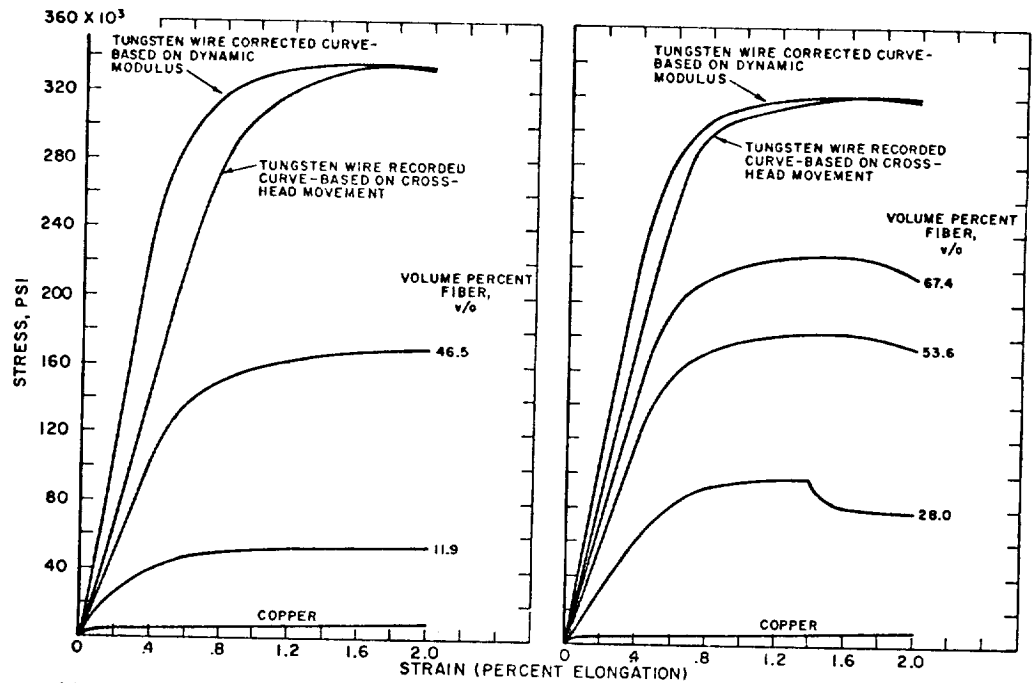
(a) For 3-mil-diameter continuous tungsten reinforcement.   (b) For 5-mil-diameter continuous tungsten reinforcement.
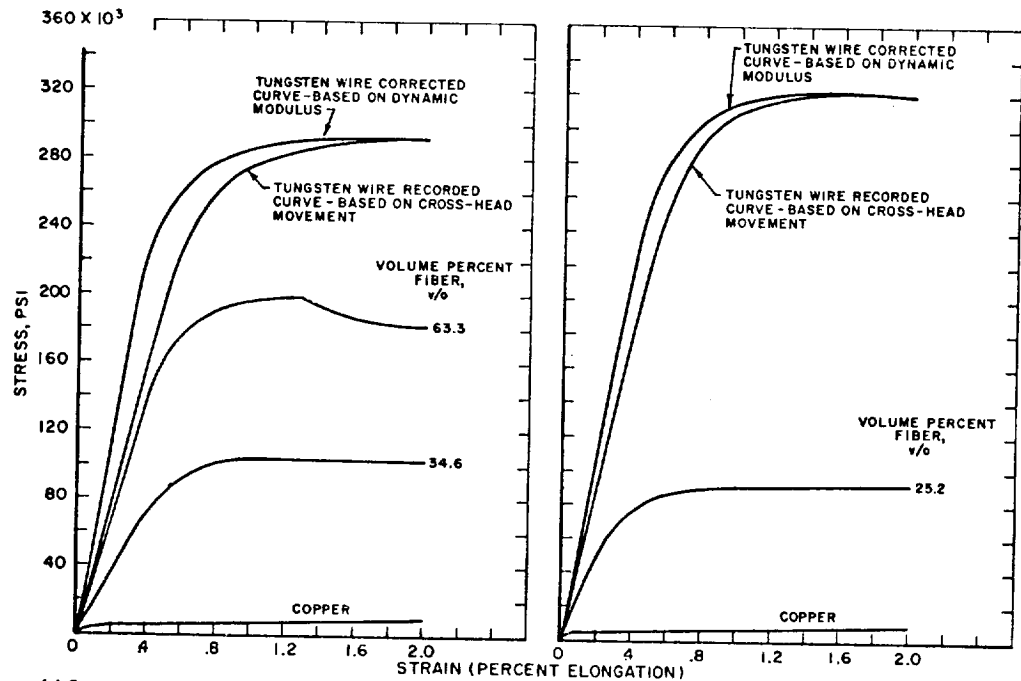
(c) For 7-mil-diameter continuous tungsten reinforcement.   (d) For 5-mil-diameter discontinuous tungsten reinforcement.

FIGURE 14.—Stress-strain curves for tungsten wire, copper, and composites reinforced with tungsten wire.

elastically, as described below:

$$E_c = E_F A_F + E_M A_M$$

where E is the initial modulus of elasticity and the subscripts c, F, and M denote composite, fiber, and matrix, respectively.

(2) As the stress increases, the matrix undergoes plastic deformation, but the fiber is still below its elastic limit. The following expression describes this behavior:

$$E'_c = E_F A_F + \left(\frac{\sigma'_M}{\epsilon}\right) A_M$$

E'_c is the secondary modulus of "elasticity" of the composite.

$$\left(\frac{\sigma'_M}{\epsilon}\right)$$

is the slope of the stress-strain curve of the matrix at a given strain.

(3) Upon application of still greater stress, the fiber is also stressed beyond its elastic limit, so that the composite deforms plastically. The behavior in this region follows the general equation:

$$\sigma_c^* = \sigma_F^* A_F + \sigma_M^* A_M$$

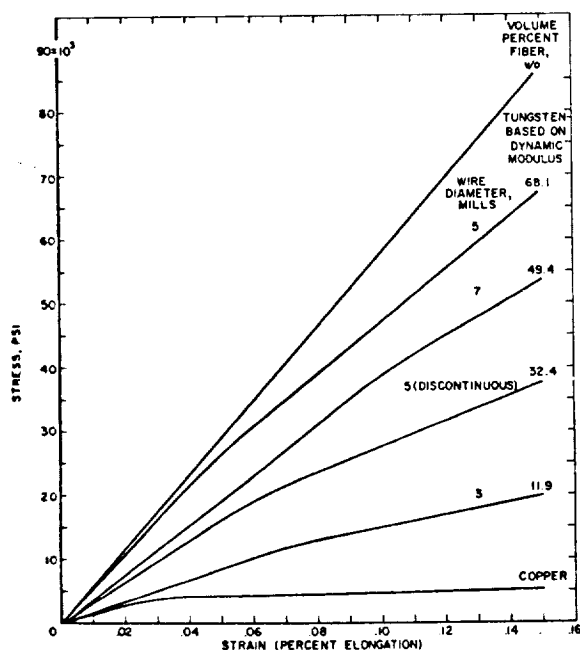FIGURE 16.—Secondary modulus of elasticity for composites reinforced with tungsten fibers.

FIGURE 15.—Enlargement of low-strain region of stress-strain curves of tungsten, copper, and composites reinforced with tungsten fibers.
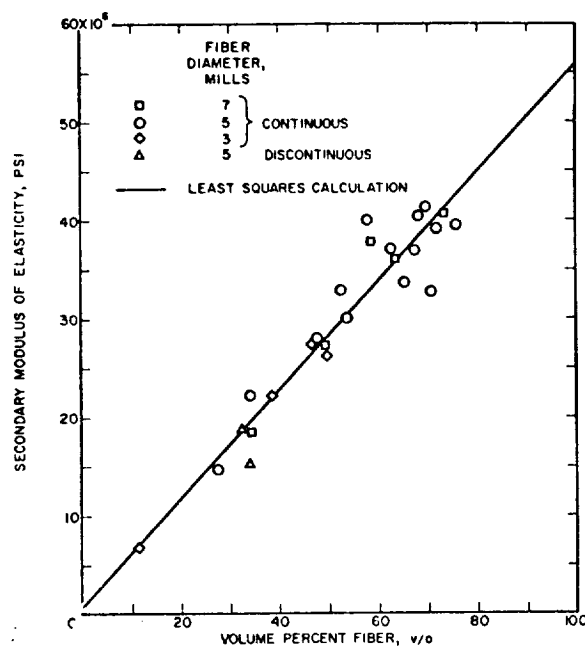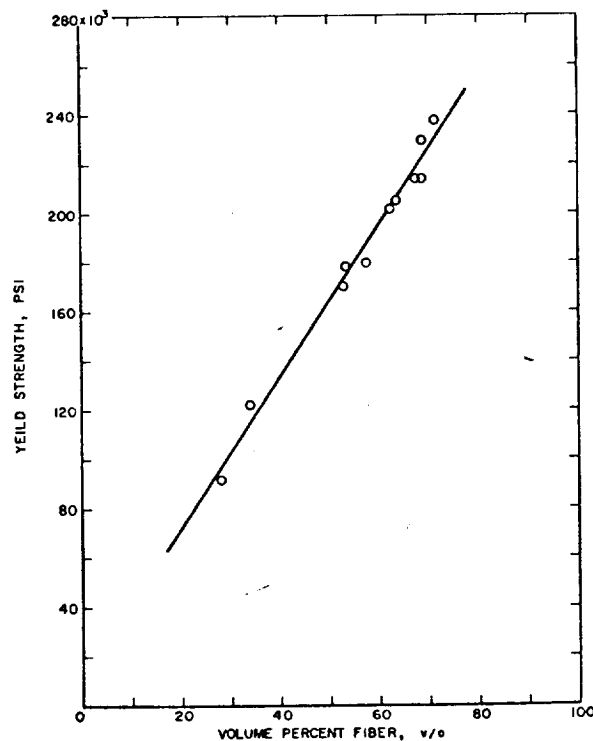

FIGURE 17.—Yield strength (based on secondary modulus) of composites reinforced with continuous 5-mil diameter tungsten fibers.

The σ^* represents stresses at any value of strain of the components.

(4) The final or fourth state is one in which the fibers break at points of weakness until an accumulation of these random fractures results in composite failure.

NASA Patent No. 3,084,421 covers composites of the type described above.[57] In addition to metal fibers, reference is also made to ceramic fibers, fibers of refractory hard metal, or whiskers of both types of materials.

Methods for positioning fibers in the matrix include electroplating, vacuum deposition, and dipping. The patent is primarily concerned with composites having a predetermined length and in which reinforcement filaments are oriented in parallel form so that their long axis coincides with the long axis of the composite. A method of making metal-reinforced composites has been described by Schuerch,[58] in which bundles of oriented fibers are placed in a tube and the tube and interstices between fibers is filled with molten metal.

BORON—ALUMINUM COMPOSITES

The general technique for boron-aluminum composites[58] is to fill a refractory tube with a bundle of aligned boron filaments and then fill the tube and interstices between the fibers with metal. In one approach, the filaments and their containers are preheated prior to infiltration with molten metal. With this process, a large percentage of the filaments form regular V-shaped cracks and the aluminum occupies them. An end-view of a boron fiber so cracked was shown in figure 2(c).

To avoid the development of this type of cracking in the boron filaments, a slight change in techniques was effective, wherein the tube packed with filaments was not preheated, but the assembly was quickly immersed in molten aluminum, evacuated, and then chilled. This procedure eliminated the V-shaped cracks, but nearly every filament had three or four fine radial cracks extending outward from the center. These cracks developed during the preparation of the

sections for microscopic examination, and similar cracks appeared in boron filaments embedded in a room-temperature-setting resin. Some boron filaments made by the vapor deposition process seemed to be under very high residual stress, which developed between the tungsten boride core and the boron overlayer.

BORON—MAGNESIUM COMPOSITES

Composites of boron filaments with a magnesium matrix have also been made by Schuerch.[58] Continuous filaments were infiltered with magnesium, using a process similar to that described above for boron-filament-aluminum, boron-aluminum composites. Properties of samples of these composites are shown in table VII. Compressive failure was observed at compressive strains of 0.7 to 0.8 percent.

COMPOSITES WITH *IN SITU* FIBERING

PROCESSING

Powder metallurgy techniques were used by Weeton et al.,[59,60,61] starting with materials listed in table VIII. Starting reagents were blended to

TABLE VII.—*Properties of Boron-Magnesium Composites*

Test Sample	1	2	3
Packing density, % of theoretical	0.52	0.71	0.52
Length of diameter ratio, in.	0.80/ 0.13	0.98/ 0.25	2.0/ 0.13
ρ, Specific weight, lb/in.^{3}	0.085	0.093	0.085
Type of loading	Compression	Compression	Bending
F^c_{ult} Ultimate composite stress, psi $\times 10^3$	188	344	* 199
Ultimate fiber stress,[b] psi $\times 10^3$	342	490	363
$\left(\dfrac{F^c_{ult}}{\rho}\right)$ Specific strength of composite, in millions of inches	2.21	3.70	2.34

* Computed from maximum bending moment, assuming linear stress distribution.

[b] Computed from observed stresses and packing density.

TABLE VIII.—*Billet Materials*

Material	Source	Nominal Purity, Weight, percent	Particle Size, μ	Melting Point, °F	Density, g/cc
Tungsten	General Electric Company	99.96	1.2	6170	91.30
Tungsten—5 volume percent hafnia	Curtiss-Wright Corporation	99.74	2.0		
Zirconia	Titanium Alloy Manufacturing Company	98.80	2.0	4892	5.49
Yttria	General Electric Company		1.7	4370	4.84
Hafnia	Wah Chang Corporation	99.92	1.9	5090	9.68
Thoria	Lindsay Light and Chemical Company		2.1	5522	10.03
Hafnium boride	The Carborundum Company	a 93.3	6.8	5880	11.20
Hafnium nitride	The Carborundum Company	b 96.6	4.6	5990	14.00
Hafnium carbide	The Carborundum Company	c 95.4	4.2	7030	12.70
Tantalum carbide	Unknown	99.85	5.0	7020	14.65

a 2.9 Percent zirconium, titanium, and carbon.
b 3.0 Percent zirconium.
c 4.6 Percent zirconium, titanium, and boron.

furnish the calculated nominal compositions in table IX. The mixing was done in jar mills at speeds and under conditions that yielded a high degree of mixing in 24 hours of rotation. Air in the jars was displaced by argon to inhibit oxidation of the powders. In a number of cases, the tungsten powder and additive mixtures were cleaned in a tower with a stream of hydrogen at 1500° F for 6 hours. The tower was heated at a rate sufficient to keep the evolved moisture below 1000 ppm.

The powders were compacted into cylinders by hydrostatically pressing at 30,000 psi. In table IX, the sintering schedules are given, where billets Nos. 1 to 7 were sintered for 4 hours at a pressure of less than 5×10^{-5} torr, at temperatures from 3500 to 4200° F. Other compacts were preheated for 2 hours in hydrogen at 2600° F, followed by a final sintering at 4200° F in a vacuum for 2 hours. This process yielded billets lower in porosity than obtained with the former method.

Most of the 2-inch diameter billets were canned in a molybdenum container having a wall thickness of 0.250 inch, using a vertical 1080-ton extrusion press. The can was prepared from molybdenum powder by pressing and sintering.

Extrusion temperatures ranging from 3700 to 4200° F were utilized. Reduction ratios were 8:1 or 16:1, and ram speeds were between 3.6 to 14.4 inches per second, as indicated in table IX. In two cases, a reduction ratio of 20:1 was used in a high-energy extrusion process at 3600° F. Several metals and other materials, such as oxides, glass, graphite, and rubber were tried as container lubricants. Oxides are effective when used to coat the die.

RESULTING FIBROUS STRUCTURES

It is most instructive to examine the microstructure of extruded products shown in figures 18 through 21. Longitudinal sections of extruded composites, having 8 to 10 volume percent of the oxides of zirconium, yttrium, hafnium, and thorium, respectively, are shown in figure 18(c), (d), (e), and (f). Figure 18(a) shows reinforced tungsten, and 18(b) is typical of the transverse sections obtained with all of the oxides. Effective fibering is evident with zirconia, yttria, and hafnia, but thorium oxide was not so effectively elongated. Aspect ratios (L/D) were 23.3 for HfO_2; 19.1 for ZrO_2; and 2.7 for yttria.

The effects with higher oxide concentrations,

TABLE IX.—*Tungsten Billet Composition and Processing*

Composition			Extrusion [a]						
Billet	Additive [b]	Amount of Additive, volume percent	Temperature, °F	Reduction Ratio	Can Material	Can Thickness, in.	Transfer Time, sec	Maximum Extrusion Pressure, lb/sq in.	Ram speed, in./sec
Vacuum-Sintered Billets									
[e] 1	----------	0	3700	8:1	Tantalum (sheet)	0.090	5	194.0×10³	6.0
							----------	----------	4.0
[e,d] 2	----------	0	4050				----------	----------	4.0
[e,d] 3	Zirconia	8.0	4200				5	183.0	5.3
[e,d] 4	Yttria	8.0	4200				----------	106.2	10.0
[e,d] 5	Hafnia	10.0	4200				6	106.0	10.0
[e] 6	Zirconia	5.0	3800	20:1					
[e] 7	Zirconia	5.0	3800	20:1					
Hydrogen-Presintered Billets [f]									
8	----------	0	4200	8:1	Molybdenum (sintered powder)	0.250	5	115.7×10³	8.6
9	----------	0		16:1	Molybdenum (sintered powder)		5	----------	------
10	----------	0		16:1	Tantalum (sheet)		----------	----------	------
11	Zirconia	14.5		8:1	Molybdenum (sintered powder)		8	79.8	14.4
12	Zirconia	20.5					5	96.8	4.8
13	Yttria	20.5					6	111.8	4.4
14	Hafnia	25.5					4.5	75.8	5.0
[g] 15	Hafnia	23.5					6	151.7	4.0
16	Thoria	8.0					4.5	89.8	4.0
17	Thoria	16.0					15	125.7	3.6
18	Hafnium boride	8.0					5	131.7	9.8
19	Hafnium nitride	8.0					5	172.6	6.6
20	Hafnium carbide	8.0					4	197.6	4.0
21	Tantalum carbide	8.0					4	173.6	9.0

[a] Billets 6 and 7 extruded in high-energy press; all others extruded in a 1000-ton conventional press.
[b] All additives mixed 24 hours with glass beads in a jar on a ball mill; isostatically pressed at 30,000 psi.
[c] Sintered in vacuum at 3500° F for 2 hours and at 4200° F for 2 hours.
[d] Powder heated in hydrogen gas stream at 1500° F for 6 hours prior to compacting.
[e] Sintered in vacuum at 4200° F for 4 hours.
[f] Presintered in hydrogen atmosphere at 2600° F for 2 hours and sintered in vacuum at 4200°F for 2 hours.
[g] Curtiss-Wright tungsten powder that contained 5 volume percent hafnia.
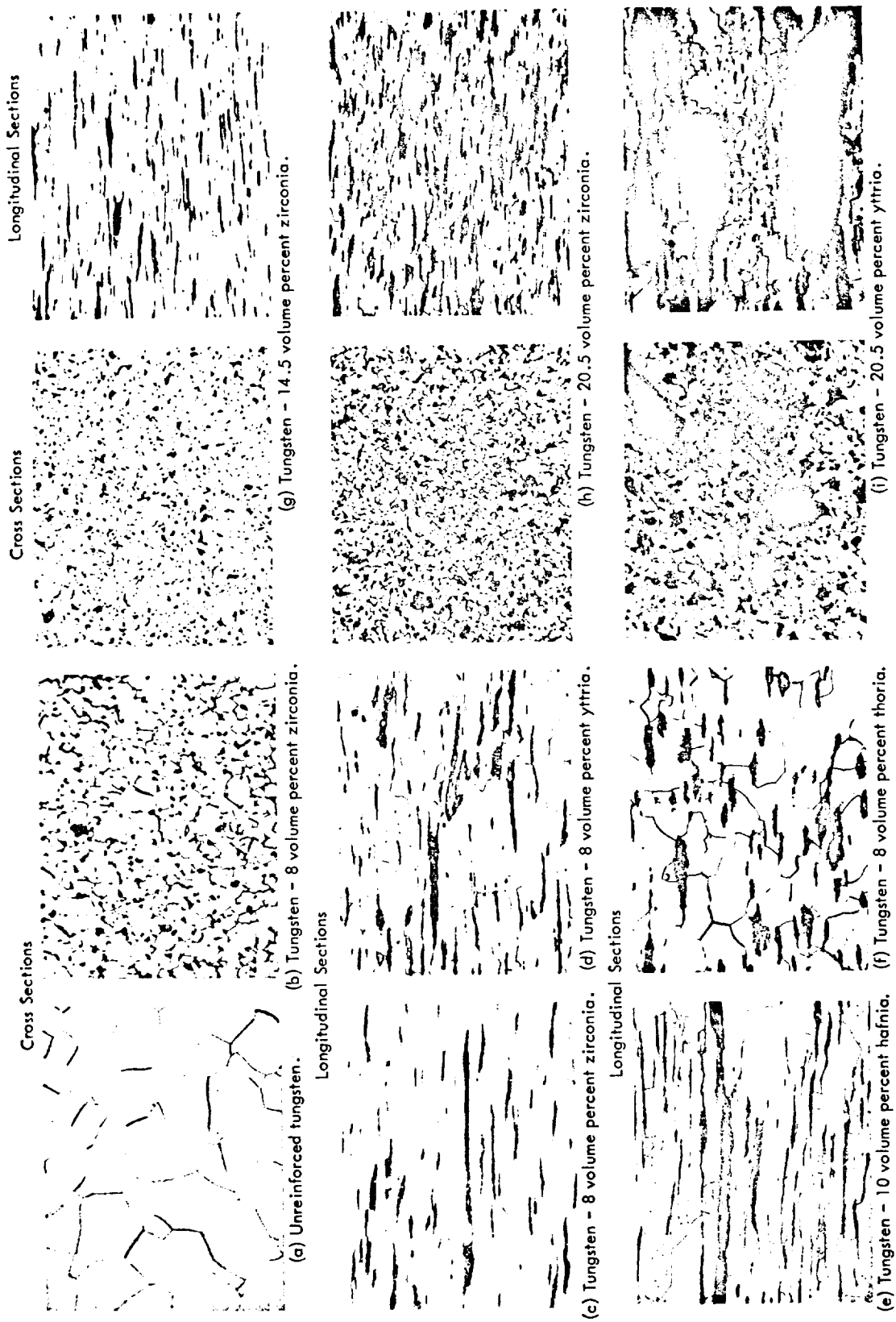
(a) Unreinforced tungsten.

(b) Tungsten – 8 volume percent zirconia.

(c) Tungsten – 8 volume percent zirconia.

(d) Tungsten – 8 volume percent yttria.

(e) Tungsten – 10 volume percent hafnia.

(f) Tungsten – 8 volume percent thoria.

(g) Tungsten – 14.5 volume percent zirconia.

(h) Tungsten – 20.5 volume percent zirconia.

(i) Tungsten – 20.5 volume percent yttria.

Cross Sections

Longitudinal Sections

FIGURE 18.—Microstructures of as-extruded tungsten and tungsten-oxide composites (500X).

Cross Sections   Longitudinal Sections

(j) Tungsten - 25.5 volume percent hafnia.

(k) Tungsten - 23.5 volume percent hafnia.

(l) Tungsten - 16 volume percent thoria.
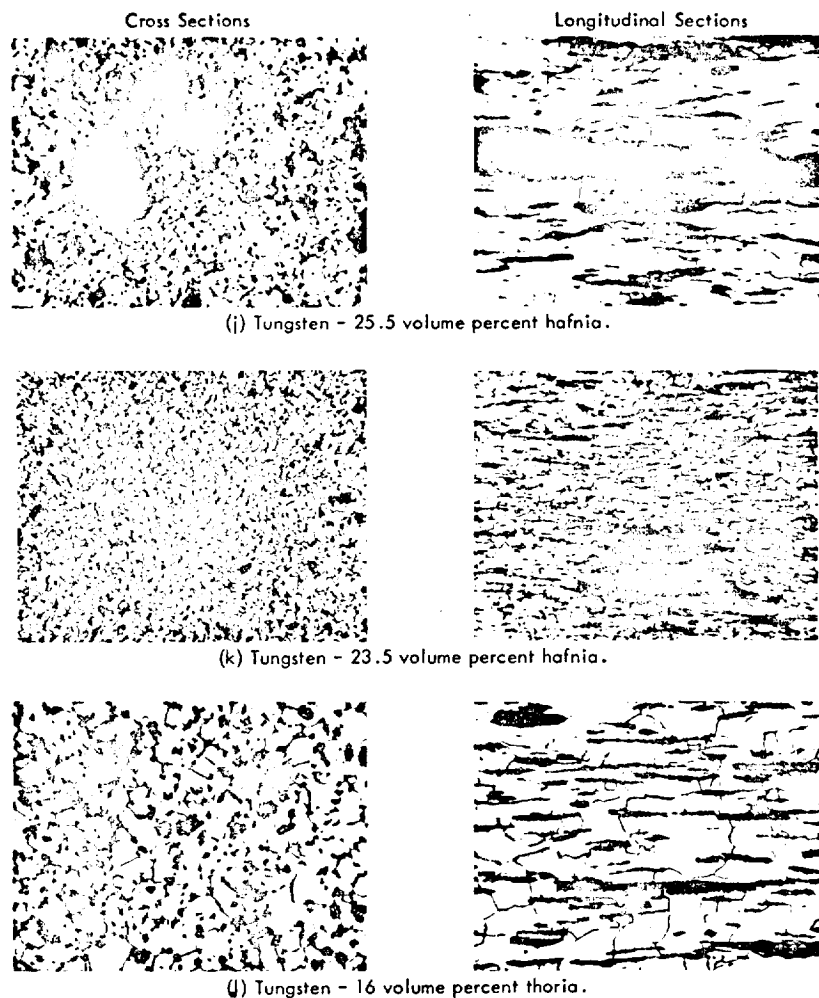
FIGURE 18.—Microstructures of as-extruded tungsten and tungsten-oxide composites (500X) (Concluded).

14.5 to 25.5 volume percent, are shown in figures 18(g) to (l). An increase in oxide concentration, up to 15 volume percent, was usually effective in increasing the extent of elongation, but additions of 20 to 25 percent resulted in excessive agglomeration.

Hafnium nitride was effectively fibered, as shown in figure 19(b), but the extent of fibering was not so good at the nose or middle sections of the extrusion. Although the refractory carbides were noticeably deformed, as shown in various sections of figure 19, no fibering was developed. However, fibering did result at the more highly deformed edges of the bar containing hafnium boride, as shown in figure 20. Figure 21 shows good examples of the effect of reduction ratio on fiber elongation.

MECHANICAL PROPERTIES

The stress-rupture lives of the composites containing 8 to 10 volume percent of additives with the most highly elongated fibers (zirconia, yttria, hafnia, and hafnium nitride) ranged from 4 to 18 times greater than that of the unreinforced matrix; however, with available information, it is not possible to determine how much of the improvement was due to fibering.

Detailed data regarding various properties of 21 different compositions after extrusion are given in table X. Of particular significance are

Cross Sections

Cross Sections

Longitudinal Sections From Nose of Extruded Bar

Longitudinal Sections From Nose of Extruded Bar

Longitudinal Sections From Middle of Extruded Bar

Longitudinal Sections From Middle of Extruded Bar

(a) Tungsten – 8 volume percent hafnium boride.

(b) Tungsten – 8 volume percent hafnium nitride.

(c) Tungsten – 8 volume percent hafnium carbide.

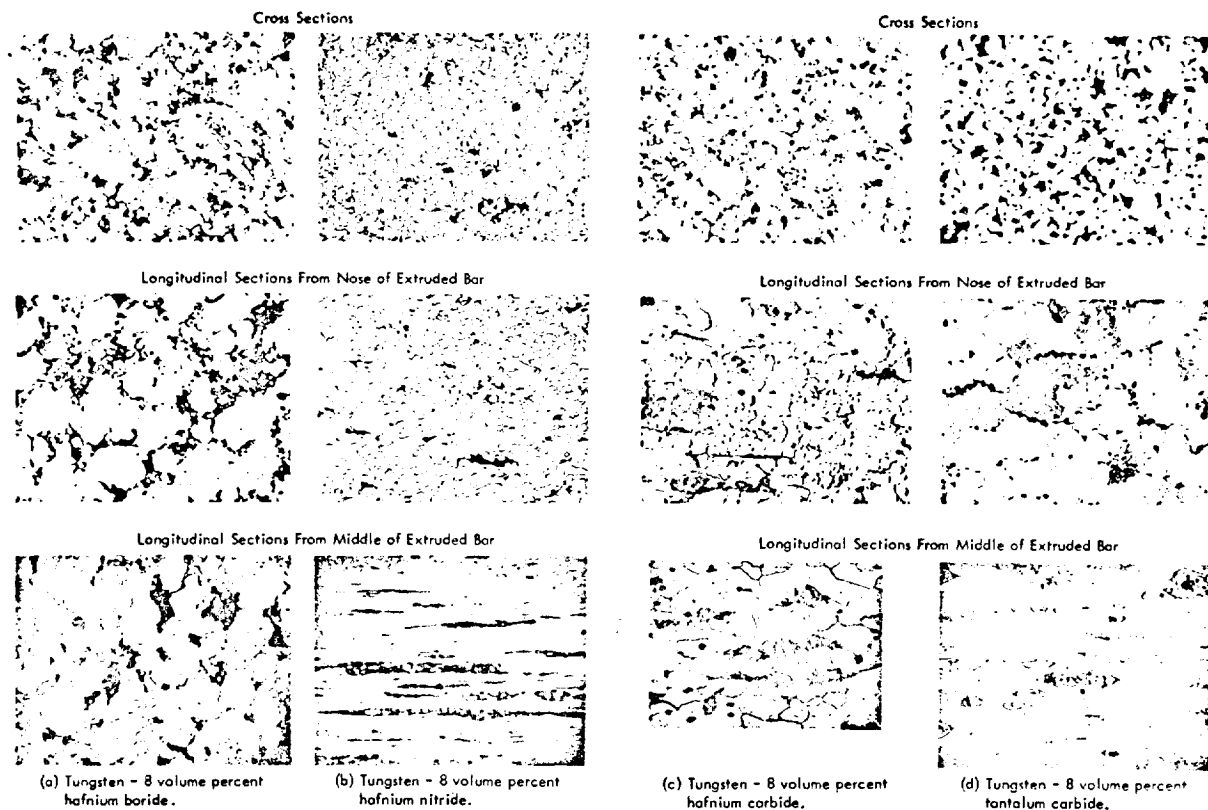(d) Tungsten – 8 volume percent tantalum carbide.

FIGURE 19.—Microstructure of as-extruded tungsten-refractory compound composites (250X).

data on stress-rupture life, illustrated by bar charts in figures 22, 23 and 24.

From figure 22 it is clear that only billets prepared with the lower concentrations of nonmetallic additives were improved by the additions. Note the low values for compositions containing 14.5 volume percent of zirconia; 20.5 percent of zirconia and yttria, respectively; and with either 23.5 or 25.5 volume percent of hafnia.

Stress at rupture for a 100-hour stress-rupture life at 3000° F, charted in figure 23, clearly indicates the value of the fibered and reacted composites. In figure 24, further details are shown for composites containing 8 volume percent of hafnium boride, hafnium nitride, and tantalum carbide, respectively, for various stress levels and temperatures.

Several tungsten-plus-additive materials produced good stress-rupture strength and creep resistance where the strength apparently was not derived from a fibrous structure. It is possible that important contributions to strength of composites result from favorable micro-stress patterns derived from the additive or its reaction products, some of which increased stress-rupture life as much as 25 to 50 fold.
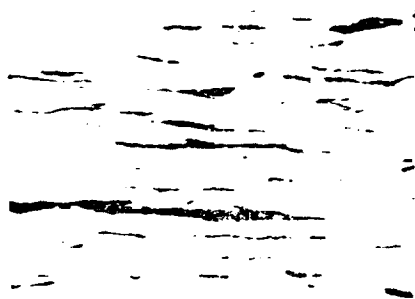
FIGURE 20.—Microstructure of tungsten-hafnium boride composite, longitudinal section (255X).
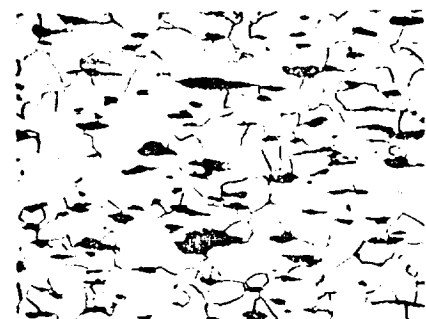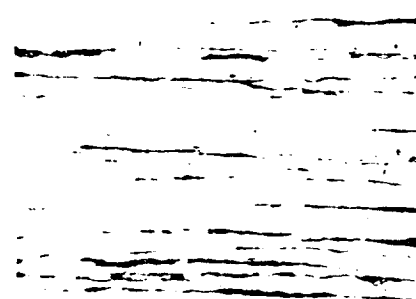
(a) Nose of bar of tungsten - 8 volume percent
    zirconia. Reduction ratio, 8:1; length-dia-
    meter ratio, 6:9.

(b) Middle of bar of tungsten - 8 volume percent
    zirconia. Reduction ratio, 8:1; length-dia-
    meter ratio, 19:1.

(c) Middle of bar of tungsten - 5 volume percent
    zirconia. Reduction ratio, 16:1; length-dia-
    meter ratio, 24:5.

(d) Middle of bar of tungsten - 5 volume percent
    zirconia. Reduction ratio, 20:1; length-dia-
    meter ratio, 29:1.

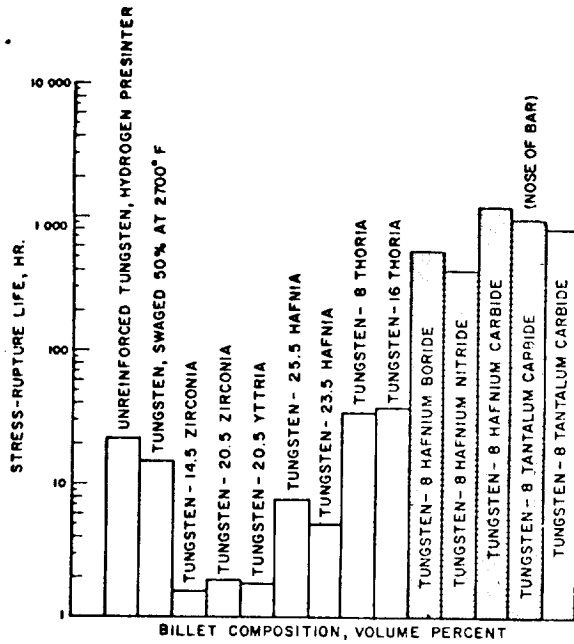FIGURE 21.—Microstructure of as-extruded tungsten-zirconia composites, longitudinal section (435X).

FIGURE 22.—Stress-rupture life of tungsten, tungsten-oxide, and tungsten-refractory compound composites (3000°F; stress—8000 lbs/sq in.).
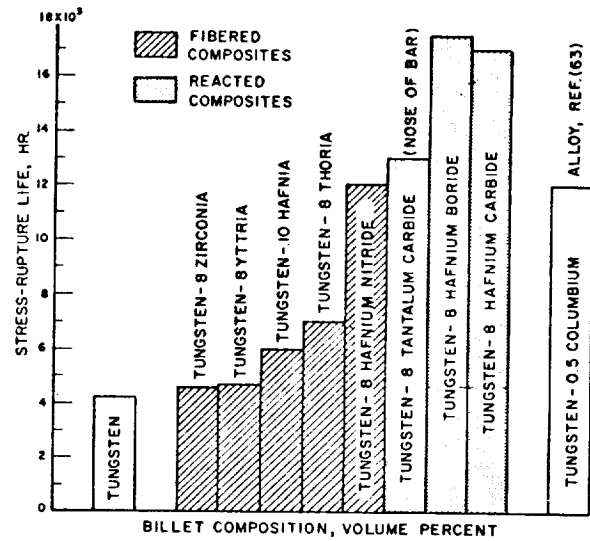
FIGURE 23.—Stress for 100-hour stress-rupture life for tungsten composites (3000°F).
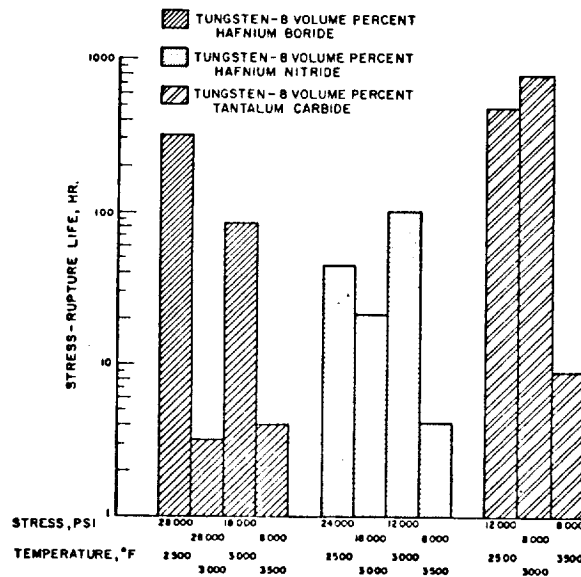

FIGURE 24.—Stress-rupture tests for tungsten—8 percent refractory compound composites (2400°F, 3000°F, and 3500°F).

TABLE X.—*Mechanical and Physical Properties of Tungsten Composites Containing Fibered and Reacted Additives*

Billet	Composition	Stress-Rupture Properties			Fiber length-Diameter Ratio	Theoretical Density, percent	Diamond pyramid hardness		Average Grain Diameter of Matrix, cm	
		Temperature, °F	Stress, psi	Stress-rupture Life, hr			Transverse	Longitudinal	Transverse	Longitudinal
1	Tungsten	3000	8 000	1.9	------	99.32	376	360	0.0040	0.0040
2	Tungsten	3000 ↓	8 000 8 000 5 000 3 000	1.5 2.6 53.8 348.7	------	99.51	383	371	0.0028	0.0045
3	Tungsten—8 volume percent zirconia	3000 3000 3000 3800	8 000 8 000 5 000 3 000	8.0 12.1 74.5 4.3	19.1	99.37	371	396	0.0016	0.0023
4	Tungsten— 8 volume percent yttria	3000 ↓ 3400 3800	8 000 8 000 7 000 6 000 4 000 3 000 3 000	7.2 9.7 23.5 44.9 161.0 25.5 1.6	12.7	99.86	401	377	0.0019	0.0025
5	Tungsten—10 volume percent hafnia	3000 3000 3000 3400	8 000 8 000 5 000 3 000	10.1 10.6 261.4 34.7	23.3	100.16	410	420	0.0022	0.0030
6	Tungsten—5 volume percent zirconia	3000 3000	8 000 8 000	4.4 3.1	12.5	99.04	------	399	--------	0.0020
7	Tungsten—5 volume percent zirconia	3000 3000 3000	8 000 8 000 8 000	3.6 4.3 5.4	29.3	99.71	------	384	--------	0.0018
8	Tungsten	3000	8 000	21.6	------	99.60	369	369	0.0047	0.0045
	Tungsten (swaged 50 percent)	3000 3000	8 000 8 000	11.8 14.7	------	--------	429	446	0.0017	0.0042
9	Tungsten	3000 3000	8 000 8 000	20.1 29.1	------	99.68	383	380	0.0023	0.0026
10	Tungsten	3000	8 000	18.9	------	--------	----	----	------	------
11	Tungsten—14.5 volume percent zirconia	3000 ↓	8 000 ↓	1.9 1.7 1.0 1.6	23.8	99.69	441	423	0.0009	0.0014
12	Tungsten—20.5 volume percent zirconia	3000 3000	8 000 8 000	2.0 1.6	10.4	ª 101.10	459	440	0.0008	0.0011
13	Tungsten—20.5 volume percent yttria	3000 3000 3000	8 000 8 000 8 000	1.7 1.3 2.4	6.8	ª 100.83	413	419	0.0009	0.0011

TABLE X.—*Concluded*

Bil-let	Composition	Stress-Rupture Properties			Fiber length-Diameter Ratio	Theoretical Density, percent	Diamond pyramid hardness		Average Grain Diameter of Matrix, cm	
		Temperature, °F	Stress, psi	Stress-rupture Life, hr			Transverse	Longitudinal	Transverse	Longitudinal
14	Tungsten—25.5 volume percent hafnia	3000 3000	8 000 8 000	8.8 6.2	14.1	ª 97.20	466	458	0.0010	0.0020
15	Tungsten—23.5 volume percent hafnia [b]	3000 ↓	8 000 ↓	4.9 4.7 4.3 5.4	16.7	ª 101.10	578	515	0.0005	0.0007
16	Tungsten—8 volume percent thoria	3000	8 000	34.2	7.8	99.22	381	389	0.0026	0.0036
17	Tungsten—16 volume percent thoria	3000	8 000	36.9	13.2	98.66	420	418	0.0012	0.0013
18	Tungsten—8 volume percent hafnium boride	3000 3000 3000 3000 3500 2500	8000 to 20 000 8 000 18 000 28 000 8 000 28 000	ᶜ 223.3 ᵈ 545.0 83.5 3.2 4.0 323.9	1.0	ª 95.63	385	425	0.0011	0.0024
19	Tungsten—8 volume percent hafnium nitride	3000 3000 3000 3000 3500 2500	8000 to 10 000 8 000 12 000 18 000 8 000 24 000	ᶜ 292.2 ᵈ 388.0 101.1 21.5 4.2 ᵉ >45.4	18.4	98.50	543	471	0.0006	0.0007
20	Tungsten—8 volume percent hafnium carbide	3000 3000 3000	8000 to 18 000 8 000 18 000	ᶜ 164.9 ᵈ 1145.0 77.9	6.6	98.19	418	406	0.0015	0.0014
21	Tungsten—8 volume percent tantalum carbide (nose of bar)	3000 3000	8000 to 14 000 8 000	ᶜ 414.6 ᵈ 920.0	------	--------	412	406	0.0012	0.0013
	Tungsten—8 volume percent tantalum carbide (middle of bar)	3000 2500	8 000 12 000	788.6 487.9	5.1	99.44	315	372	0.0011	0.0033

ª Questionable because of changes in theoretical density.
[b] 18.5 volume percent hafnia was added to Curtiss-Wright tungsten powder already containing 5 volume percent hafnia.
ᶜ Total time with increasing load (see table IV).
ᵈ Estimated time from creep data in table IV.
ᵉ Test incomplete; specimen support rod on stress-rupture machine failed.

References

1. MACHLIN, E. S.: "Non-Metallic Fibrous Reinforced Metal Composites," Materials Research Corporation Status Report, Contract NOw 61-0209-c (1961).
2. BASKEY, R. H.: "Fiber Reinforcement of Metallic and Non-Metallic Composites," Clevite Corp. Report, Contract AF33(657)-7139, Part I, (1962); Part II (1963).
3. KELLEY, A. and DAVIES, G. J.: "The Principles of Fiber Reinforcement of Metals," Metallurgical Reviews, vol. 10, No. 1, pp. 1–77 (1965).
4. CRATCHLEY, D.: "Experimental Aspects of Fiber-Reinforced Metals," Metallurgical Reviews, vol. 10, No. 37, pp. 79–144 (1965).
5. THOMAS, A. G., HUFFADINE, J. A., and MOORE, N. C.: "Preparation, Properties and Application of Metal/Ceramic Mixtures," Metallurgical Reviews, vol. 8, No. 32, pp. 461–488 (1963).
6. CARROLL-PORCZYNSKI, C. Z.: "Advanced Materials," Astex Publishing Corp., Guilford, Surrey (1962).
7. TINKELPAUGH, J. R., and CRANDALL, W. B. (Editors): "Cermets," Reinhold Publishing Corp., New York, and Chapman and Hall, London (1960).
8. BLOCH, E. A.: "Dispersion Strengthened Aluminum Alloys," Metallurgical Reviews, vol. 6, No. 22, pp. 193–239 (1961).
9. ANON: "Strong New Nickel Beats Superalloys Above 2000°F," Materials in Design Engineering, vol 56, No. 2, pp. 12–13 (1962).
10. HANSEN, N. and LILHOLT, H.: "Bibliography on Dispersion-Strengthened Materials," Risö Report No. 48, Roskilde, Denmark, Danish Atomic Energy Commission (1962).
11. HOFFMAN, G. A.: "The Structural Exploitation of the Strength of Whiskers," Rand Corp. Report, No. P-1149, p. 13 (Aug. 6, 1957).
12. HERRING, C. and GALT, J.: "Elastic Properties of Very Small Metal Specimens," Phys. Rev., vol. 85, No. 6, p. 1060 (1952).
13. BRENNER, S. S.: "Growth and Perfection of Crystals," (Ed.: Doremus, R. H., et al.) John Wiley, New York (1958).
14. COLEMAN, R. V.: "The Growth and Properties of Whiskers," Metallurgical Reviews, vol. 9, No. 35, pp. 261–304 (1964).
15. MORELY, J. G.: "Strong Fibers and Fiber-Reinforced Metals," Proc. Roy. Soc., vol 282A, No. 1388, p. 43 (1964).
16. DASH, W. C.: "Growth and Perfection of Crystals," John Wiley, New York, p. 189 (1958).
17. MORLEY, J. G. and PROCTOR, B. A.: "Strength of Sapphire Crystals," Nature, vol. 196, No. 4859, p. 1082 (1962).
18. PEARSONS, G. L., READ, W. T., and FELDMAN, W. L.: "Deformation and Fracture of Small Silicon Crystals," Acta Met., vol. 5, No. 4, pp. 181–191 (1957).
19. POLANYI, N.: "Nature of the Breaking Process," Z. Physik., vol. 7, pp. 323–327 (1921).
20. ERCKER, L.: "Treatise on Ores and Assaying," (1574, Second Edition 1580), Translated by Sisco, A. G. and Smith, C. S., University of Chicago, p. 177 (1951).
21. GILMAN, J. J. (Ed.): "The Art and Science of Growing Crystals," John Wiley, New York (1963).
22. NADGORNYI, E. M.: "Properties of Filament Crystals," USP. Fiz. Nauk., vol. 77, pp. 201–227 (1962); Chem. Abs., vol. 57, 15913h (1962).
23. HARDY, H. K.: "Progress in Metal Physics," vol. IV, Pergamon Press, London, p. 45 (1956).
24. BREWER, L. and SEARCY, A. W.: "The Gaseous Species of the Al–Al₂O₃ System," J. Amer. Chem. Soc., vol. 73, pp. 5308–14 (Nov. 1951).
25. CUNNINGHAM, ANDREW L., BEASLEY, ROBERT M., and WAINER, EUGENE: "Mechanism of Growth and Physical Properties of Refractory Oxide Fibers," For Office of Naval Research, Washington, D.C., U.S. Department of Commerce, Office of Tech. Service, P.B. Rept. No. 171520 (1960).
26. BLAKELY, J. M. and JACKSON, K. A.: "Growth of Crystal Whiskers," Jour. Chem. Physics, vol. 37, pp. 428–30 (1962).
27. WAGNER, R. S. and ELLIS, W. C.: "Vapor-Liquid-Solid Mechanism of Single Crystal Growth," Appl. Phys. Letters, vol. 4, No. 5, pp. 89–90 (Mar. 1964).
28. BURTON, W. K., CABRERA, N., and FRANK, F. C.: "The Growth of Crystals and Equilibrium Structure of Their Surfaces," Trans. Roy. Soc., London, vol. A243, pp. 299–358 (1951).
29. FORTY, A. J. and FRANK, F. C.: "Growth and Slip Patterns on the Surfaces of Crystals of Silver," Proc. Roy. Soc., London, vol. A217, pp. 262–270 (1953).
30. ESHELBY, J. D.: "Tentative Theory of Metallic Whisker Growth," Phys. Rev., vol. 91, No. 3, pp. 755–756 (1953).
31. PRICE, P. B., VERMILYEA, D. A., and WEBB, M. B.: "The Growth and Properties of Electrolytic Whiskers," Acta. Met., vol. 6, pp. 524–531 (1958).
32. ATEN, A. H. W. and BOERLAGE, MISS LOUISE M.: "The Crystallization of Metals by Galvanic Precipitation and Certain Related Phenomena," Rec. Trav. Chim. Pays-Bas, vol. 39, pp. 720–735 (1920).

43

33. GUNTER-SCHULZE, A.: "Crystalline Deposition of Metals by Electrolysis with High Current Densities," I. Lead. Z. Electrochem., vol. 28, pp. 119-122 (1922).

34. VERMILYEA, D. A.: "The Theory of Electrolytic Crystal Growth," Jour. Chem. Phys., vol. 25, pp. 1254-1263 (1956).

35. PFEFFERKORN, GERHARD: "Electron-Microscopic Investigation of Metal Oxide Layers," Z. Metallkunde, vol. 46, pp. 204-207 (1955).

36. HARMAN, C. G.: "Nonglassy Ceramics as Fibers," Ceramic Industry, p. 74 (July 1959).

37. ANON: "Nonmetallic Composites," Chemical Week, p. 83 (Aug. 21, 1965).

38. McDANELS, D. L., JECH, R. W., and WEETON, J. W.: "Fiber Reinforced Composites," Composite Materials and Structures Proc., Sixth Sagamore Ordnance Materials Conference, pp. 116-143 (Aug. 18-21, 1959).

39. McDANELS, D. L., JECH, R. W., and WEETON, J. W.: "Metals Reinforced with Fibers," Metal Progress, vol. 78, No. 6, pp. 118-121 (1960).

40. WEETON, J. W.: "Fiber Reinforced Metallic Composites," (In Press.)

41. WEETON, J. W. and SIGNORELLI, R. A.: "Fiber-Metal Composites," Presented to the Twelfth Sagamore Army Materials Conference (Aug. 24-27, 1965).

42. HARMAN, C. G.: "New Concept Provides Basis for Developing Improved Ceramics," Ceram. Ind. (Aug. 1959).

43. COTTRELL, A. H.: "Strong Solids," Proc. Roy. Soc., vol. 282A, No. 1388, pp. 2-9 (1964).

44. GATTI, A., CREE, R., FEINGOLD, E., and MEHAN, R.: "The Synthesis of Boron Carbide Filaments," Final Report, Contract NASw-670, Space Sciences Laboratory, Missile and Space Division, General Electric Company (July 10, 1964).

45. GATTI, A., CREE, R., MEHAN, R., and MANCUSO, C.: "Study of Growth Parameters Involved in Synthesizing Boron Carbide Filaments," First Quarterly Report, Prepared for NASA under Contract NASw-937, Space Sciences Laboratory, Missile and Space Division, General Electric Company (Sept. 1964).

46. GATTI, A. and MANCUSO, C.: "Study of the Growth Parameters Involved in Synthesizing Boron Carbide Filaments," Second Quarterly Report, Prepared for NASA under Contract NASw-937, Space Sciences Laboratory, Missile and Space Division, General Electric Company, Philadelphia, Pennsylvania (Dec. 1964).

47. GATTI, A., MANCUSO, C., FEINGOLD, E., MEHAN, R., and CREE, R.: "Study of Growth Parameters Involved in Synthesizing Boron Carbide Filaments," Prepared for NASA under Contract NASw-937, Space Sciences Laboratory, Missile and Space Division, Philadelphia, Pennsylvania (Apr. 1965).

48. ROBINS, H. E. and GILES, P. W.: "The High Tempera-ture Vaporization Properties of Boron Carbide and the Heat of Sublimation of Boron," J. Phys. Chem., vol. 68, pp. 983-985 (1964).

49. WITUCKI, ROBERT M.: "Boron Filaments," NASA Contractor Report No. NASA CR-96, Prepared under Contract No. NASw-652 by Astro Research Corporation (Sept. 1964).

50. TALLEY, C. P.: "Boron Reinforcements for Structural Composites," ASD-TDR-62-257 (Mar. 15, 1962).

51. GATES, L. E., JR. and LENT, W. E.: "Refractory Glass Fibers," Work Conducted under Contract NAS 8-50 for George C. Marshall Space Flight Center of NASA, Presented at 67th Annual Meeting of the American Ceramic Society, Philadelphia, Pennsylvania (May 4, 1965).

52. PETRASEK, D. W. and WEETON, J. W.: "Alloying Effects on Tungsten-Fiber-Reinforced Copper-Alloy or High-Temperature-Alloy Matrix Composites," NASA TN D-1568 (Oct. 1963).

53. McDANIELS, D. L., JECH, R. W., and WEETON, J. W.: "Stress-Strain Behavior of Tungsten-Fiber-Reinforced Copper Composites," NASA TN D-1881 (Oct. 1963).

54. PETRASEK, D. W. and WEETON, J. W.: "Effects of Alloying on Room Temperature Tensile Properties of Tungsten-Fiber-Reinforced-Copper Alloy Composites," Transactions of the Metallurgical Society of AIME, vol. 230, pp. 977-990 (Aug. 1964).

55. McDANELS, D. L., JECH, R. W., and WEETON J. W.: "Analysis of Stress-Strain Behavior of Tungsten-Fiber-Reinforced Copper Composites," Transactions of the Metallurgical Society of AIME, vol. 233, pp. 636-642 (Apr. 1965).

56. McDANELS, D. L., JECH, R. W., and WEETON, J. W.: "Preliminary Studies—Fiber Reinforced Metallic Composites," Woodside Panel on Composite Materials, ASM, Chicago, Ill., (Nov. 2, 1959).

57. McDANELS, DAVID L., JECH, ROBERT W., WEETON, JOHN W., and PETRASEK, DONALD W.: "Reinforced Metal Composites," U.S. Patent No. 3,084,421 (Apr. 9, 1963).

58. SCHUERCH, H.: "Compressive Strength of Boron-Metal Composites," NASA CR-202, Prepared under Contract No. NASw-652 by Astro Research Corporation (Apr. 1965).

59. WEETON, JOHN W., McDANELS, DAVID L., JECH, ROBERT W., OLDRIEVE, ROBERT E., PETRASEK, DONALD W., and SIGNORELLI, ROBERT A.: "Method of Making Fiber Reinforced Metallic Composites," U.S. Patent No. 3,138,837 (June 30, 1964).

60. QUATINETZ, MAX, WEETON, JOHN W., and HERBELL, THOMAS P.: "Studies of Tungsten Composites Containing Fibered or Reacted Additives," NASA-TN D-2757 (Apr. 1965).

61. BARTH, V. D.: "Review of Recent Developments in the Technology of Tungsten," DMIC Memo No. 139 (Nov. 24, 1961).